

Selective Inhibitors of G2019S-LRRK2 Kinase Activity

Albert W. Garofalo,* Jessica Bright, Stéphane De Lombaert, Alyssa M. A. Toda, Kerry Zobel, Daniele Andreotti, Claudia Beato, Silvia Bernardi, Federica Budassi, Laura Caberlotto, Peng Gao, Cristiana Griffante, Xinying Liu, Luisa Mengatto, Marco Migliore, Fabio Maria Sabbatini, Anna Sava, Elena Serra, Paolo Vincetti, Mingliang Zhang, and Holly Carlisle



Cite This: <https://dx.doi.org/10.1021/acs.jmedchem.0c01243>



Read Online

ACCESS |



Metrics & More

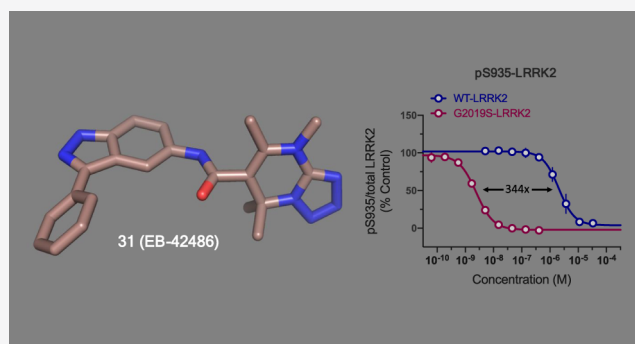


Article Recommendations



Supporting Information

ABSTRACT: Pathogenic variants in the leucine-rich repeat kinase 2 (LRRK2) gene have been identified that increase the risk for developing Parkinson's disease in a dominantly inherited fashion. These pathogenic variants, of which G2019S is the most common, cause abnormally high kinase activity, and compounds that inhibit this activity are being pursued as potentially disease-modifying therapeutics. Because LRRK2 regulates important cellular processes, developing inhibitors that can selectively target the pathogenic variant while sparing normal LRRK2 activity could offer potential advantages in heterozygous carriers. We conducted a high-throughput screen and identified a single selective compound that preferentially inhibited G2019S-LRRK2. Optimization of this scaffold led to a series of novel, potent, and highly selective G2019S-LRRK2 inhibitors.



INTRODUCTION

Parkinson's disease (PD) is the most common form of parkinsonism and the second most common age-related neurodegenerative disease. It is estimated to affect about 1% of the population over age 65 with prevalence increasing with increasing age. It is a chronic disease marked by progressive disability and diminished quality of life. PD is characterized by motor symptoms that include resting tremor, rigidity, postural instability, impaired speech, and bradykinesia, which are predominantly driven by loss of dopaminergic neurons in the substantia nigra pars compacta. Non-motor symptoms including hyposmia, dysautonomia, and changes in sleep, cognition, and mood also occur with varying frequency. Current therapeutic strategies for PD are largely focused on controlling motor symptoms with dopamine replacement and by enhancing the activity of the remaining dopaminergic neurons. At present, no disease-modifying therapies exist that address the underlying neuropathological drivers of disease; this remains a significant unmet medical need for PD patients.

It has long been known that family members of PD patients have an increased risk of developing the disease compared to the general population. In 2004, variants in the leucine-rich repeat kinase 2 (LRRK2) gene were shown to co-segregate with disease in familial PD.¹ LRRK2 is a large, multidomain protein that is unusual for having two functional enzymatic domains: a Ras-like GTPase domain and a serine–threonine kinase domain. At least seven dominantly inherited pathogenic

variants within LRRK2 have been identified. Of these, the G2019S variant occurring within the kinase domain is the most common, accounting for 4% of familial PD and up to 1% of apparently sporadic PD worldwide.² Interestingly, while some of the pathogenic variants are found within the kinase domain, all pathogenic variants have been reported to show increased autophosphorylation at S1292 when expressed in cells,³ implicating abnormal kinase activity as the likely cause of pathogenicity. LRRK2 kinase inhibition has therefore become a promising therapeutic strategy for PD, and several small-molecule LRRK2 kinase inhibitors are currently in clinical development.

While the therapeutic potential of LRRK2 kinase inhibitors is clear, this strategy is complicated by the potential for on-target safety liabilities associated with the loss of physiological LRRK2 activity. It has been found that LRRK2 has a role in mouse kidney and lung homeostasis, as implied in knockout and kinase-dead mutants.⁴ Genetic knockout of LRRK2 in rodents causes vacuolization in specific cell types in kidney and lung, suggesting that normal LRRK2 plays a critical and

Received: July 31, 2020

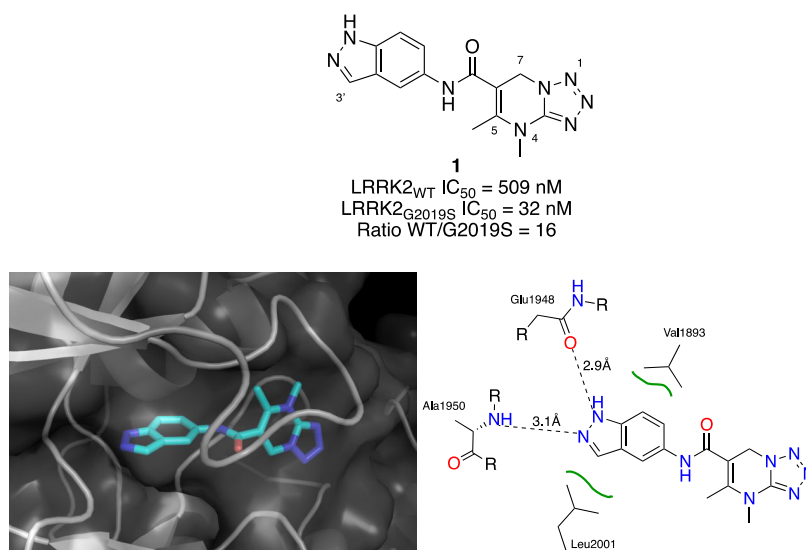


Figure 1. Homology model of the LRRK2 kinase domain depicting compound **1** docked into the ATP pocket. Principal hydrogen-bonding interactions involve both N-1 and N-2 of the indazole.

nonredundant role in vesicular trafficking in those cell types in rodents.⁵ Supporting these interpretations, pharmacological inhibition of LRRK2 kinase activity in rodents causes morphological changes in type II pneumocytes of the lung and proximal tubules in the kidney that are similar to those observed in knockout animals.⁶ In nonhuman primates, strong inhibition of LRRK2 kinase activity also causes vacuolization in lung cells, although the effect is reversible and without apparent functional consequence over the duration tested.⁷ However, the safety risks associated with chronic LRRK2 kinase inhibition in humans cannot be fully assessed without long-term clinical observation. Because the majority of PD patients carrying the LRRK2-G2019S variant are heterozygous,⁸ a precision medicine approach of selectively targeting only the pathogenic activity while sparing the physiological LRRK2 activity could offer efficacy and safety advantages for this patient population.

RESULTS AND DISCUSSION

We conducted a high-throughput screening campaign searching for inhibitors of G2019S-LRRK2 kinase activity on a 50K compound subset of the Aptuit library that was prioritized based on ligand efficiency.⁹ This set had generally lower molecular weight and better CNS multiparameter optimization (MPO) scores¹⁰ as compared with the overall collection. Compounds that met a specified potency threshold in the primary screen were progressed to IC₅₀ determination in an 11-point biochemical concentration–response assay against both wild-type (WT) and G2019S-LRRK2 to confirm potency and assess selectivity. Out of this effort emerged indazole **1**, the single hit that exhibited a preference for inhibiting the G2019S mutant protein over WT protein by >10-fold.

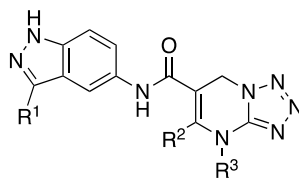
Lacking an X-ray crystal structure of LRRK2, we constructed a proprietary homology model of the kinase domain based on chimeric Aurora kinase A crystal structures where point mutations were introduced to mimic the LRRK2 hinge and glycine-rich loop regions combined. Mutated residues in the chimera included L210M, Y212L, P214S, and L215K in the hinge region and R137Q, P138L, K141D, K143S, and N146S in the glycine-rich loop. The homology model based on this chimera was then optimized to accommodate SAR observa-

tions. While not all of the structure–activity relationships described below were predicted by this model, certain aspects of the SAR were consistent with the general pose.

Docking compound **1** in our homology model suggested that the indazole binds to the hinge, as shown in Figure 1. This pose agreed with our expectations as indazole is a privileged structure for kinase inhibitors and numerous crystal structures containing indazole ligands bound in the ATP site of kinases are available in the protein data bank (PDB). In the majority of these structures, the indazole functions as a hinge binder as demonstrated with the known LRRK2 inhibitor MLi-2.¹¹ In our model, N-1 of the indazole hydrogen bond donates to Glu1948 and N-2 accepts a hydrogen bond from Ala1950 within the ATP pocket. Our confidence in this binding mode was bolstered by the complete loss of activity upon *N*-methylation of the indazole or replacement of the indazole with benzo[*d*]isoxazole (not shown). This binding pose suggested that substituents at the indazole C-3' position would be partially solvent-exposed and might therefore be used to modulate the properties of an inhibitor series. As shown in Table 1, substitution of the available valence at C-3' (R¹) was tolerated and afforded a number of subnanomolar inhibitors. The addition of a methyl group (**2**) tripled the potency while maintaining selectivity. Larger groups afforded potencies of less than a nanomolar. The lower limit of reliable quantification of potency in the biochemical assay was ~0.2 nM, and therefore, the actual IC₅₀ values for **4**, **6**, and **7** on G2019S-LRRK2 were likely lower than 0.2 nM. For compound **4**, potency against both mutant and WT was such that selectivity could not be accurately determined in the biochemical assays. In general, the preferred substitution at C-3' tended to be an aromatic or heteroaromatic ring as demonstrated with analogues **3**–**7**. Other substituents such as bromine (**8**), carboxamide (**9**), and benzoylamine (**10**) also improved potency relative to compound **1**. However, not all substituents at C-3' were found to increase potency, as is apparent with butanoylamine **11**.

We also varied the methyl substituents on the dihydrotriazolopyrimidine during our initial investigations. Removal of the C-5 methyl as in compound **12** completely abolished activity on both WT and G2019S-LRRK2. Single carbon

Table 1. Biochemical Inhibitory Potency and Selectivity of C-7-Unsubstituted 4,7-Dihydro-1H-tetrazolo[1,5-a]pyrimidines



Cmpd	R ¹	R ²	R ³	IVB WT IC ₅₀ (nM) ^a	IVB G2019S IC ₅₀ (nM) ^a	IVB Ratio WT/G2019S
1	H	Me	Me	509	32	16
2	Me	Me	Me	121	10	12
3		Me	Me	9.0	0.44	20
4		Me	Me	< 0.2	< 0.2	ND
5		Me	Me	0.88	0.40	2.2
6		Me	Me	0.70	< 0.2	> 3.5
7		Me	Me	0.53	< 0.2	> 2.6
8	Br	Me	Me	96	2.4	40
9	CONH ₂	Me	Me	125	6	21
10	NHCOPh	Me	Me	108	3	35
11	NHCO <i>n</i> -Pr	Me	Me	> 10000	1190	> 8.4
12	H	H	Me	> 10000	> 10000	ND
13	H	Et	Me	534	244	2.2
14	H	Me	Et	865	58	15
15	H	Me		6130	4650	1.3
16	H	Me	CONMe ₂	888	53	17
17	H	Me	Ph	5.7	2.6	2.2
18	H	Me	Ac	2540	513	5.0

^aIn vitro biochemical (IVB) potency values are the geometric mean of a minimum of two IC₅₀ values determined in independent experiments. ND = not determined.

homologation at C-5 (compound 13) also had a detrimental effect on potency, as well as the preference for G2019S inhibition over WT. Similarly, homologation to the *N*-ethyltetrazolopyrimidine (compound 14) decreased potency; however, in this case, selectivity was preserved. Though additional substituents were tried at N-4 (R³), none exhibited an improved combination of potency and selectivity over the methyl group found in 1 (*cf.* compounds 15–18).

In an effort to better understand key interacting elements in these inhibitors, we examined the role of the amide by preparing the *N*-methylamide 19 and thioamide 20 (Figure 2). *N*-Methylation of the amide resulted in complete loss of activity, suggesting a potentially important hydrogen-bonding

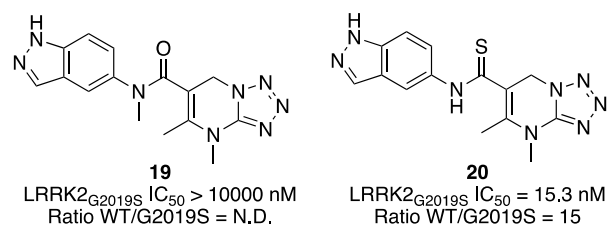
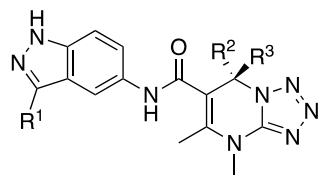


Figure 2. Amide substitutions.

interaction with the amide NH occurring within the binding pocket. Of course, other factors such as a change in molecular conformational or an unfavorable steric interaction cannot be

Table 2. Biochemical Inhibitory Potency and Selectivity of C-7-Substituted 4,7-Dihydro-1H-tetrazolo[1,5-a]pyrimidines



Cmpd	R ¹	R ²	R ³	IVB WT IC ₅₀ (nM) ^a	IVB G2019S IC ₅₀ (nM) ^a	IVB Ratio WT/G2019S
21	H	H	Me	71	1.64	43
22	H	Me	H	302	94	3.2
23	Me	H	Me	20	0.82	24
24	Me	Me	H	1220	51	24
25		H	Me	< 0.2	< 0.2	ND
26		H	Me	< 0.2	< 0.2	ND
27		Me	H	1.0	< 0.2	> 5
28	H	Me	Me	1300	12	108
29	Me	Me	Me	152	0.8	190
30		Me	Me	0.3	< 0.2	> 1.5
31	Ph	Me	Me	6.6	< 0.2	> 33

^aIn vitro biochemical (IVB) potency values are the geometric mean of a minimum of two IC₅₀ values determined in independent experiments. ND = not determined.

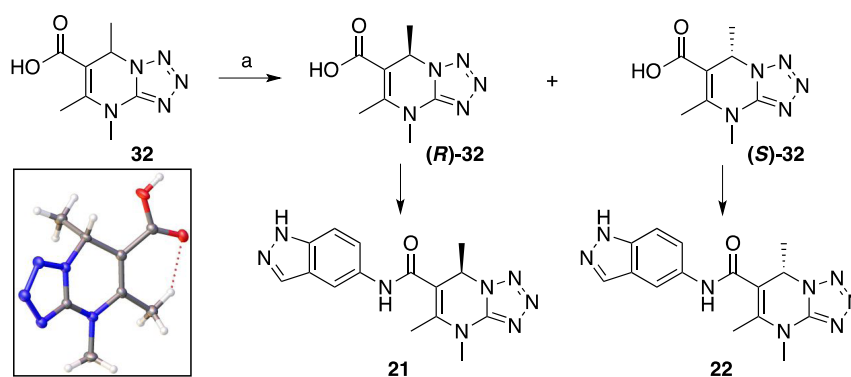


Figure 3. Determination of absolute stereochemistry from chiral carboxylic acids. (a) Chiral HPLC separation using an (R,R)-Whelk-O 1 column (25 cm × 2 cm), 10 μm, eluting with 40:60 *n*-hexane:EtOH.

ruled out. Since thioamides are known to be weaker hydrogen bond acceptors than amides,¹² the lack of any reduction in activity observed for compound **20** coupled with maintenance of selectivity for G2019S-LRRK2 inhibition suggested that the carbonyl oxygen is not involved in critical hydrogen bonding.

We further elaborated the dihydro-tetrazolopyrimidine by incorporating substituents at C-7 (R² and R³), as shown in

Table 2. Addition of a single methyl group at C-7 of (*R*)-configuration, compound **21**, improved inhibition of both WT and G2019S-LRRK2 but most importantly increased the G2019S over WT selectivity to 43-fold. The (*S*)-enantiomer, **22**, had the opposite effect on both potency and selectivity. The same pattern with respect to potency was also observed with compounds **23** and **24**. The previously demonstrated

increases in potency with 3-(pyridin-4-yl) and 3-(2-morpholinopyridin-4-yl) indazole were preserved in compounds **25**–**27**, although biochemical selectivity could not be accurately determined due to the above-described assay limitations.

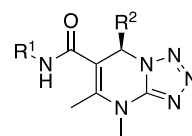
The synthesis of compounds **21**–**27** employed commercially available, racemic 4,7-dihydro-4,5,7-trimethyltetrazolo[1,5-*a*]-pyrimidine-6-carboxylic acid (**32**), which was separated into its individual enantiomers by chiral high-performance liquid chromatography (HPLC). To determine the absolute configuration of these inhibitors, we prepared **21** and **22** from the resolved carboxylic acids. A small-molecule X-ray crystallographic analysis of the carboxylic acid used to prepare the eutomer, **21**, was obtained and indicated the (*R*)-stereochemistry assigned to this compound (Figure 3).

We also looked at geminal substitution on the dihydropyrimidine, which afforded compounds with greatly increased preference for inhibition of the G2019S protein. As shown in Table 2, compound **28** is 108-fold more potent against G2019S-LRRK2 than WT. The selectivity obtained with geminal substitution appears to result from decreased affinity for binding in the WT ATP-binding pocket rather than a significantly increased affinity for the G2019S ATP-binding pocket. As before, adding substituents to the indazole, as in compounds **29**–**31**, boosted the potency of these inhibitors. In the case of compound **29**, methyl substitution at the indazole C-3 afforded a subnanomolar inhibitor with 190-fold selectivity. Aryl substituted compounds, **30** and **31**, were too potent in our assay to gauge their biochemical selectivity. However, selectivity of these two analogues was confirmed by cellular activity assays (vide infra).

During the course of our investigations, we also evaluated the effects of replacing the indazole with other known hinge binders and related bicycles (Table 3). Replacing the indazole with either indole, as in compound **33**, or benzimidazole, compound **34**, resulted in complete loss of activity against both WT and G2019S-LRRK2. Imidazopyridines **35** and **36** were also ineffective replacements for indazole (*cf.* compound **2**) as was indolinone **37**. Interesting results were observed with benzimidazolones **38**–**40**. Analogue **38** exhibited >36-fold selectivity but lost potency relative to compound **1**. Alkylation of the cyclic urea afforded compounds with quite different profiles. Analogue **39** lost all activity against both WT and G2019S-LRRK2, likely due to an unfavorable steric interaction with the hinge, while analogue **40** was both potent against G2019S-LRRK2 and very selective. Phthalimide **41** had a potency and selectivity profile similar to **40**, as did isoindolinone **42**. The most successful indazole replacement was 1-aminoisoquinoline. Compound **43** had equivalent selectivity compared with compound **21** with a G2019S-LRRK2 IC_{50} = 12 nM.

We profiled a number of these inhibitors for potency and selectivity in cellular assays (Table 4). Inhibition of phosphorylation at two sites on LRRK2, S935, and S1292 was measured in HEK293 cell lines stably overexpressing human WT or G2019S-LRRK2. S1292 is an autophosphorylation site that is positively correlated with LRRK2 kinase activity.¹³ Although this is not the case with S935, which is more highly phosphorylated on the inactive fraction of LRRK2 in cells, S935 nonetheless becomes dephosphorylated in response to inhibitor binding and is therefore a useful pharmacodynamic marker.¹⁴ Inhibitor IC_{50} values determined using pS935 and pS1292 on G2019S-LRRK2 were well correlated. For WT-LRRK2, IC_{50} values measured on pS935

Table 3. Biochemical Potency and Selectivity of LRRK2 Inhibitors with Alternative Hinge Binders



Cmpd	R ¹	R ²	IVB WT IC ₅₀ (nM) ^a	IVB G2019S IC ₅₀ (nM) ^a	IVB Ratio WT/G2019S
33		H	> 10000	> 10000	ND
34		H	> 10000	> 10000	ND
35		H	> 10000	3120	> 3.2
36		H	> 10000	1350	> 7.4
37		H	> 10000	6370	> 1.6
38		H	> 8600	240	> 36
39		Me	> 10000	> 10000	ND
40		Me	2870	58	49.7
41		Me	2840	55	52
42		Me	1700	32	53
43		Me	581	12	48

^aIn vitro biochemical (IVB) potency values are the geometric mean of a minimum of two IC_{50} values determined in independent experiments. ND = not determined.

were consistently higher than those measured on pS1292, resulting in a trend toward greater selectivity on pS935.

Inhibition of LRRK2 phosphotransferase activity to an endogenously expressed substrate, Rab10, was assessed for three of the most potent and selective inhibitors (**23**, **30**, and **31**) in cell lines overexpressing either WT-LRRK2 or G2019S-LRRK2 (Table 4). Potency and selectivity in the pThr-Rab10 assay were well aligned with the inhibition of pS935-LRRK2 in the same cell lines. Compound **31** (EB-42486) exhibited a WT/G2019S selectivity ratio of >300-fold on pS935-LRRK2 and on the substrate pThr73-Rab10 (Figure 4). In contrast, the nonselective inhibitor, MLi-2 (Figure 4), showed no preference for the G2019S-LRRK2 variant. The level of selectivity exhibited by compound **31** is remarkable, given that G2019S-LRRK2 differs from WT-LRRK2 by only a single

Table 4. Cellular Potencies for Inhibition of pS935-LRRK2, pS1292-LRRK2, and pThr73-Rab10

cmpd	pS935-LRRK2 ^b			pS1292-LRRK2 ^c			pThr73-Rab10 ^d		
	WT IC ₅₀ (nM) ^a	G2019S IC ₅₀ (nM) ^a	ratio WT/G2019S	WT IC ₅₀ (nM) ^a	G2019S IC ₅₀ (nM) ^a	ratio WT/G2019S	WT IC ₅₀ (nM) ^a	G2019S IC ₅₀ (nM) ^a	ratio WT/G2019S
4	377	8.3	45	74.4	9.2	8	ND	ND	ND
7	3300	21	157	242	21	12	ND	ND	ND
21	>10 000	189	>53	2180	104	21	ND	ND	ND
23	5220 (8743) ^e	46.1 (106) ^e	113 (82) ^e	380	19	20	9736	137	71
25	1140	14.7	78	272	12.1	22	ND	ND	ND
26	65	2.4	27	20.9	1.2	18	ND	ND	ND
30	145 (259) ^e	1.1 (1.5) ^e	132 (173) ^e	33.7	1.0	34	473	4.7	101
31	1060 (2092) ^e	3.1 (2.5) ^e	339 (837) ^e	117	1.7	71	3924	11.4	344

^aCellular potencies are reported as the geometric mean of a minimum of two IC₅₀ values determined in independent experiments. ^bPotency on pS935-LRRK2 was measured with a fluorescence resonance energy-transfer (FRET)-based assay. ^cpS1292-LRRK2 was measured with a Meso Scale Discovery (MSD) electrochemiluminescence assay. ^dpThr73-Rab10 inhibition was measured with an immunoblot-based assay. ^epS935 IC₅₀ and selectivity values shown in parentheses were determined with an immunoblot-based assay performed on the same cell lysates that were evaluated in the pThr73-Rab10 assay. ND = not determined.

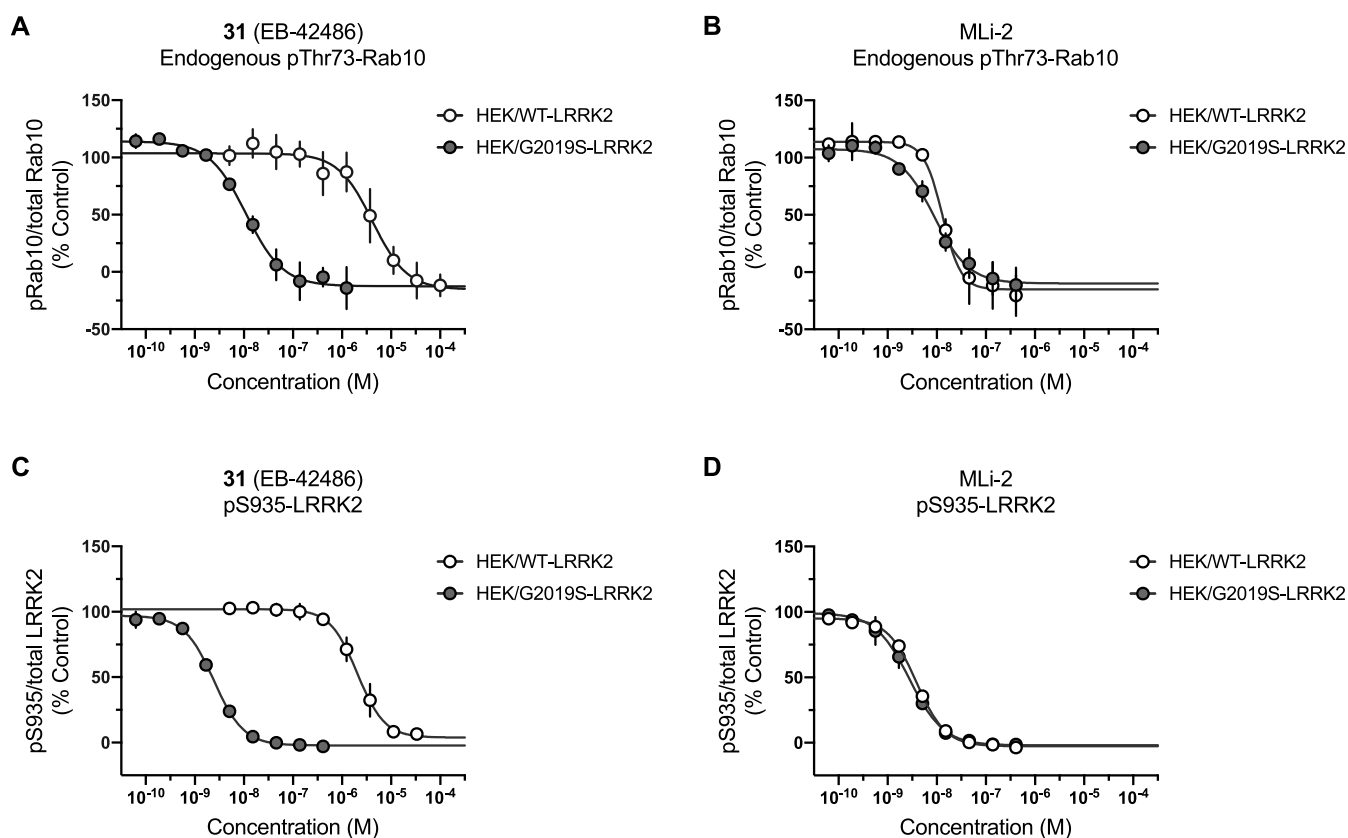


Figure 4. Inhibition of pThr73-Rab10 in HEK293 cell lines overexpressing either WT-LRRK2 or G2019S-LRRK2. (A) Compound 31 inhibited phosphorylation of the LRRK2 substrate, Rab10, 344-fold more potently in the G2019S-LRRK2 overexpression line (IC₅₀ = 11.4 ± 1.1 nM, *n* = 3) compared to that in the WT-LRRK2 overexpression line (IC₅₀ = 3,924 ± 1.6 nM, *n* = 3). (B) MLI-2 showed similar potency on pThr73-Rab10 in both cell lines (HEK/G2019S-LRRK2 IC₅₀ = 8.5 ± 1.3 nM, *n* = 3; HEK/WT-LRRK2 IC₅₀ = 12.5 ± 1.1 nM, *n* = 3). (C) Compound 31 inhibited pS935-LRRK2 837-fold more potently in the G2019S-LRRK2 line (IC₅₀ = 2.5 ± 1.1 nM, *n* = 3) compared to that in the WT-LRRK2 line (IC₅₀ = 2,092 ± 1.4 nM, *n* = 3). (D) MLI-2 showed similar potency on pS935-LRRK2 in both cell lines (HEK/G2019S-LRRK2 IC₅₀ = 2.8 ± 1.2 nM, *n* = 3; HEK/WT-LRRK2 IC₅₀ = 3.9 ± 1.1 nM, *n* = 3). Potency is reported as the geometric mean of IC₅₀ values ± geometric standard deviation. Error bars show standard deviation.

amino acid within the ATP-binding pocket. This compound was also profiled at 100 nM (>500-fold biochemical G2019S IC₅₀) against a panel of 409 kinases using a commercial, active site-directed competition binding assay to determine its kinase selectivity. Even at this high concentration relative to its on-target potency, compound 31 exhibited impressive

kinome selectivity in this panel, with only six kinases being highly inhibited: HPK1, JNK1, JNK2, JNK3, TTK, and YSK4.

In general, the compounds described herein were found to have disappointing *in vitro* absorption, distribution, metabolism, and excretion (ADME) properties (e.g., low solubility, substrates for efflux transporters). However, it was desirable to

develop in vitro–in vivo correlations during the early stage of our explorations, and based on the exceptional potency and selectivity for G2019S-LRRK2 measured in cellular activity assays, analogue **31** was selected for pharmacokinetic (PK) profiling in CD-1 mice (summarized in Table 5). Following a

Table 5. Pharmacokinetic Parameters of 31 (EB-42486) in Fasted CD-1 Mice

parameter	IV administration ^a (0.5 mg/kg)	oral administration ^b (2 mg/kg)
AUC ($\mu\text{M}/\text{h}$)	0.528 \pm 0.023	0.847 \pm 0.060
C_{max} (μM)	0.615 \pm 0.029 ^c	0.299 \pm 0.024
T_{max} (h)		0.50 \pm 0.0
$T_{1/2}$ (h)	0.87 \pm 0.09	1.85 \pm 0.07
MRT (h)	1.14 \pm 0.12	2.89 \pm 0.11
Cl (mL/min/kg)	38.1 \pm 1.7	
F (%)		40.1

^aDosed as a solution of the free base (0.25 mg/mL) in a mixture of dimethyl sulfoxide (DMSO), solutol, and water (5:5:90). ^bDosed as a fine suspension of the free base (0.2 mg/mL) in a mixture of DMSO, solutol, and water (5:5:90). ^cInitial concentration. MRT, mean residence time; F , bioavailability.

single 2 mg/kg oral dose in fasted mice, a mean maximum plasma concentration of 0.299 μM was measured approximately 30 min post dose. The mean residence time (MRT) after oral dosing was 2.89 h. The compound exhibited moderate clearance, which was commensurate with an IV half-life of 0.87 h, and reasonable oral bioavailability of ~40% was observed. Bioanalytical assessment of brain tissue after 2 mg/kg oral dosing showed no compound exposure in the brain. This observation was consistent with in vitro experiments in MDCKII-MDR1 cells indicating that **31** is subject to P-glycoprotein-mediated efflux.

Synthetic Chemistry. Compounds **1** and **2** were prepared by coupling commercially available aminoindazoles with carboxylic acid **49**. Compounds **3–5**, **7–8**, and **13–17** were prepared as shown for compound **3** in Scheme 1. Suzuki–Miyaura cross-coupling of 3-bromo-5-nitroindazole (**44**) with 4-pyridylboronic acid, followed by reduction of the nitro group afforded aminoindazole **46**. Separately, the Biginelli reaction¹⁵ was employed to form tetrazolo[1,5-*a*]pyrimidine **48**, which was hydrolyzed to give carboxylic acid **49**. T3P-mediated

coupling of aminoindazole **46** and carboxylic acid **49** afforded inhibitor **3**. Compounds **6** and **9–11** were prepared as shown in Scheme 2 for compound **6**. Compound **18** was prepared as shown in Scheme 3. Ester **48** was treated with allyl bromide and hydrolyzed to give carboxylic acid **53**. Coupling of **53** with 1*H*-indazol-5-amine followed by deprotection and acylation gave **18**.

The *N*-methylamide, **19**, and the thioamide, **20**, were prepared as shown in Schemes 4 and 5. Amide bond coupling between 5-methylamino indazole, **56**, and carboxylic acid **49** gave **19** and treatment of compound **1** with Lawesson's reagent afforded **20**.

Compounds **21–25** were prepared by coupling either (*R*)-**32** or (*S*)-**32** with commercially available 5-aminoindazoles.

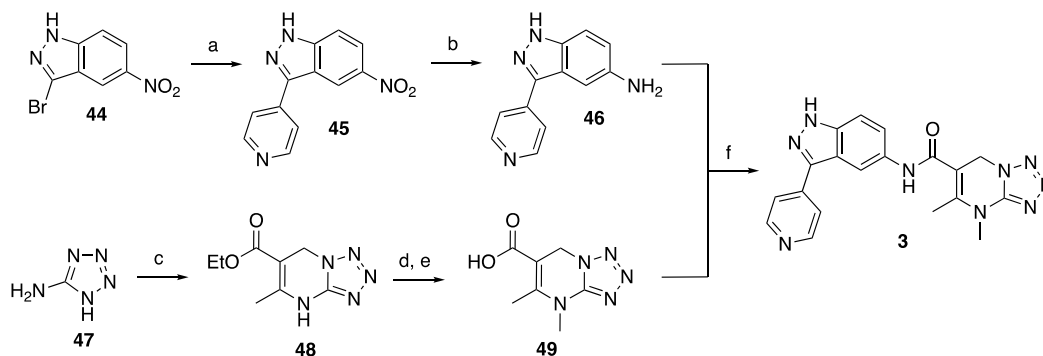
The synthesis of compounds **26** and **27** is shown in Scheme 6. The pinacolborane, **58**, was prepared in two steps from 3-bromo-5-nitro-1*H*-indazole (**44**). Suzuki–Miyaura cross-coupling with 4-(4-bromopyridin-2-yl)morpholine followed by nitro group reduction gave amine **60**. Amide bond coupling with (*R*)-**32** afforded **61**. Treatment of **61** with 4 M HCl successfully removed the SEM protecting group but also caused racemization of the chiral center. The enantiomeric pairs, **26** and **27**, were then isolated using chiral chromatography.

The gem-dimethyl-4,7-dihydro-tetrazolopyrimidines **28–31** were prepared as shown for compound **28** in Scheme 7. Condensation of aminotetrazole with methyl 2-acetyl-3-methyl-2-butenolate afforded tetrazolopyrimidine **64**. *N*-Methylation with MeI followed by LiOH hydrolysis gave carboxylic acid **66**, which was coupled with *N*-(1)-Boc-5-aminoindazole and deprotected to afford compound **28**.

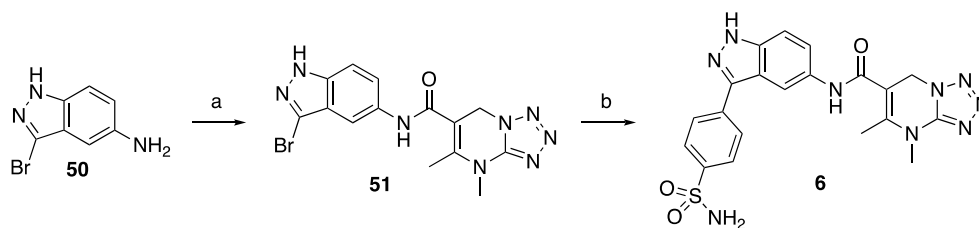
Compounds **33**, **34**, **37**, **38**, **39**, and **40** were similarly prepared using commercially available amine and carboxylic acid (*R*)-**32**. Compound **35** was prepared as shown in Scheme 8. Bromination of 2-methyl-5-nitropyridine (**68**) gave bromide **69**. Formation of amine **70** with NH_4OH followed by cyclization with Ac_2O and nitro group reduction afforded 3-methylimidazo[1,5-*a*]pyridin-6-amine (**72**), which was then coupled with carboxylic acid **49** to yield compound **35**.

Compound **36** was prepared as shown in Scheme 9 starting from 4-bromopyridine-2-carbonitrile (**73**). Grignard addition followed by concomitant reduction of the imine with NaBH_4 gave amine **74**. Formation of the formamide and cyclization

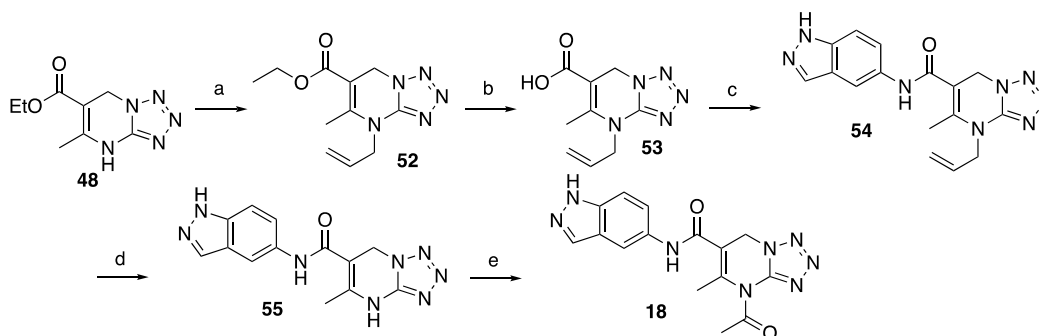
Scheme 1. Synthesis of Inhibitor 3^a



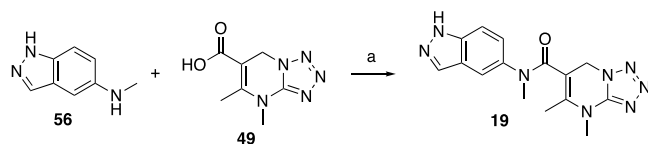
^aReagents: (a) 4-pyridylboronic acid, KOAc, Pd(amphos)Cl₂, EtOH, 100 °C; (b) Zn, NH_4Cl , EtOH, 80 °C, 56%, two steps; (c) EtOAc, formaldehyde (37 wt % in H_2O), AcOH, EtOH, 120 °C, microwave, 62%; (d) MeI, Cs_2CO_3 , 50 °C; (e) LiOH, EtOH, tetrahydrofuran (THF), H_2O , 55 °C, 59%, two steps; and (f) T3P, EtOAc, Et_3N , 15 °C or 1-ethyl-3-(3-dimethylaminopropyl)carbodiimide (EDCI), pyridine, 30 °C, 5%.

Scheme 2. Synthesis of Inhibitor 6^a

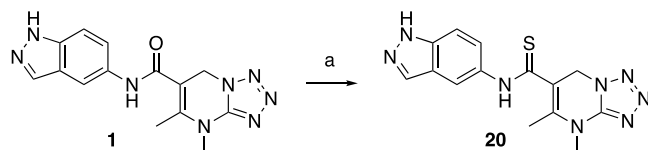
^aReagents: (a) 49, T3P, Et₃N, EtOAc, 60 °C, 16%; and (b) (4-sulfamoylphenyl)boronic acid, Pd(PPh₃)₄, Na₂CO₃, *N,N*-dimethylformamide (DMF), H₂O, 100 °C, 16%.

Scheme 3. Synthesis of Inhibitor 18^a

^aReagents: (a) allyl bromide, NaH, THF, 15 °C, 27%; (b) LiOH·H₂O, EtOH, H₂O, 15 °C, 66%; (c) 1*H*-indazol-5-amine, T3P, EtOAc, Et₃N, 20 °C, 50%; (d) 1,3-dimethylbarbituric acid, Pd(PPh₃)₄, DCM, EtOH, 55 °C, 57%; and (e) CH₃COCl, Et₃N, DCM, 15 °C, 6%.

Scheme 4. Synthesis of *N*-Methyl Amide 19^a

^aReagents: (a) 1-[bis(dimethylamino)methylene]-1*H*-1,2,3-triazolo[4,5-*b*]pyridinium 3-oxide hexafluorophosphate (HATU), DMF, Et₃N, 21%.

Scheme 5. Synthesis of Thioamide 20^a

^aReagents: (a) Lawesson's reagent, dioxane, 18 h, 100 °C, 3%.

with POCl₃ gave imidazopyridine 76. Coupling of 76 with amide 77 afforded compound 36.

The synthesis of compound 43 is summarized in Scheme 10. Boc protection of 6-nitroisquinolin-1-amine (78) followed by reduction of the nitro group, coupling with carboxylic acid (*R*)-32, and deprotection yielded target 43.

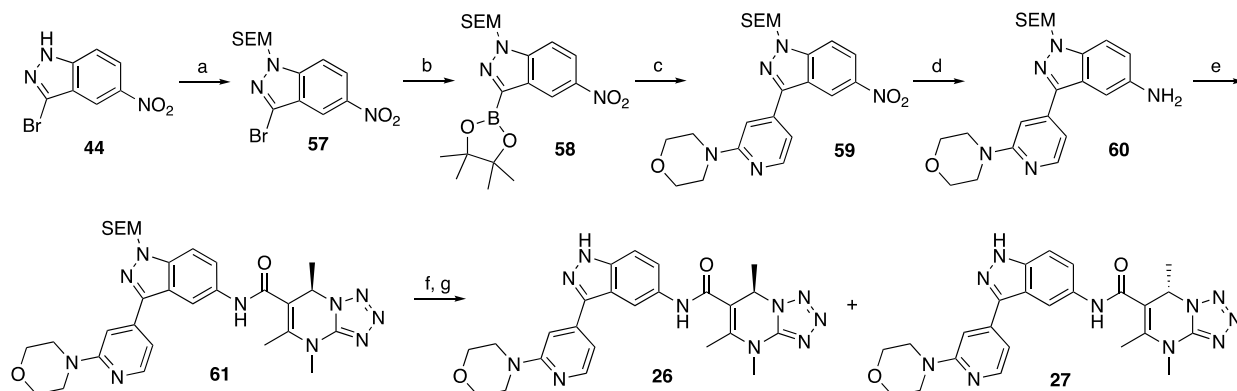
CONCLUSIONS

Our efforts to find G2019S-LRRK2 selective inhibitors for a targeted therapeutic approach in a genetically defined PD patient population have resulted in the discovery of compound 31 (EB-42486). Employing a ligand-based drug design approach starting from a single HTS hit led to a series of potent and highly selective G2019S-LRRK2 inhibitors, as

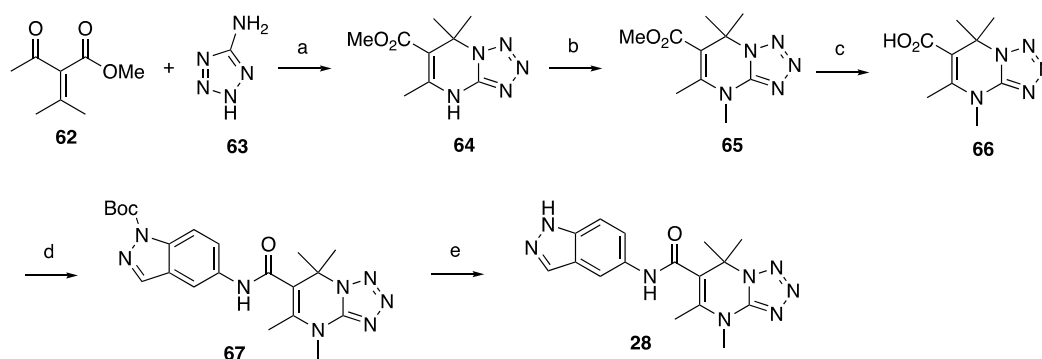
measured in a biochemical and confirmed by several cellular assays. To the best of our knowledge, this is the first identification of small molecules that can precisely target a prominent pathogenic mutation in LRRK2. Though only a single amino acid within the ATP-binding pocket differentiates WT from G2019S-LRRK2, selectivity of >200-fold for biochemical kinase activity and >300-fold for cellular activity on an endogenously expressed substrate have been demonstrated. While compounds disclosed herein were found to be poorly brain-penetrant, the initial SAR emerging from the investigation of this class of compounds constitutes a promising starting point for the continued, focused development of additional G2019S-LRRK2 selective compounds with improved pharmacokinetic properties.

EXPERIMENTAL SECTION

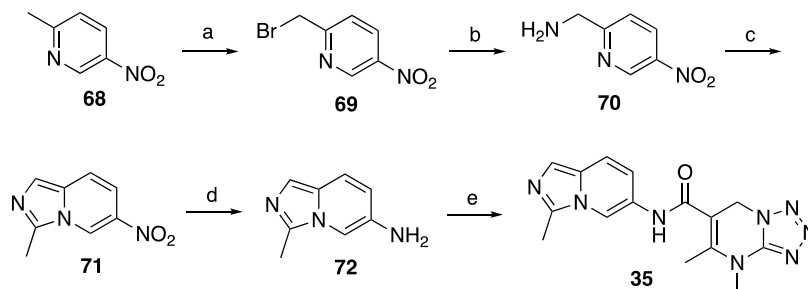
Materials and Methods. Reagents and solvents were obtained from commercial sources and used as supplied. ¹H NMR spectra were recorded on either a Bruker Avance 400, a Bruker Avance III 400, or an Agilent Direct Drive spectrometer. The spectra were acquired in the stated solvent, and chemical shifts (δ) are reported in ppm relative to the residual solvent peak. Chemical shifts are given in parts per million using conventional abbreviations for designation of major peaks, e.g., s, singlet; d, doublet; t, triplet; q, quartet; dd, doublet of doublets; dt, doublet of triplets; br, broad. Mass spectrometry was performed using an ultraperformance liquid chromatography/mass spectrometry (UPLC/MS) Acquity™ system equipped with a PDA detector and coupled to a Waters single quadrupole mass spectrometer. Where thin-layer chromatography (TLC) has been used, R_f is the distance traveled by the compound divided by the distance traveled by the solvent on a TLC plate. Chiral SFC separation was performed using a Thar SFC Prep 80 instrument and a Phenomenex Lux Cellulose-2 column (250 mm × 25 mm, 10 μm). Purities of all target compounds were greater than 95% as determined by HPLC analysis. Compounds were analyzed for and found not to contain pan assay interference (PAINS) substructural features.

Scheme 6. Synthesis of Inhibitors 26 and 27^a

^aReagents: (a) SEM-Cl, NaH, DMF, 0 °C - r.t., 60%; (b) bis(pinacolato)diboron, KOAc, 1,4-dioxane, Pd(dppf)Cl₂, 100 °C; (c) 4-(4-bromopyridin-2-yl)morpholine, Cs₂CO₃, THF, water, Pd(dppf)Cl₂, 100 °C, 44%, two steps; (d) NH₄Cl, Fe, EtOH, water, 80 °C, 80%; (e) (R)-32, Et₃N, HATU, DMF, 0 °C - r.t., 33%; (f) 4 M HCl, dioxane, THF, r.t., 18%; and (g) chiral chromatography.

Scheme 7. Synthesis of Inhibitor 28^a

^aReagents: (a) EtOH, 4 Å molecular sieves, reflux, 56%; (b) MeI, Cs₂CO₃, DMF, 97%; (c) LiOH, THF; (d) *N*-(1)-Boc-5-aminoindazole, HATU, Et₃N, DMF, r.t.; and (e) trifluoroacetic acid (TFA), DCM, 0 °C - r.t., 4%, three steps.

Scheme 8. Synthesis of Inhibitor 35^a

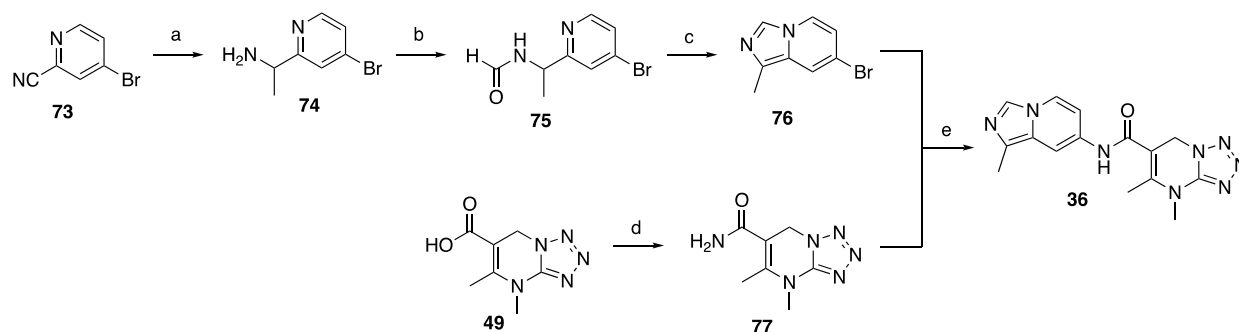
^aReagents: (a) 2-methyl-5-nitropyridine, *N*-bromosuccinimide (NBS), benzoyl peroxide, CCl₄, 80 °C, 31%; (b) NH₄OH, dioxane, 25 °C; (c) Ac₂O, PTSA, 100 °C, 32%, two steps; (d) H₂, 10% Pd/C, MeOH, 25 °C; and (e) 49, HATU, *i*-Pr₂NEt, DMF, 25 °C, 16%, two steps.

All experiments utilizing animals were conducted under protocols approved by the WuXi Institutional Animal Care and Use Committee (IACUC).

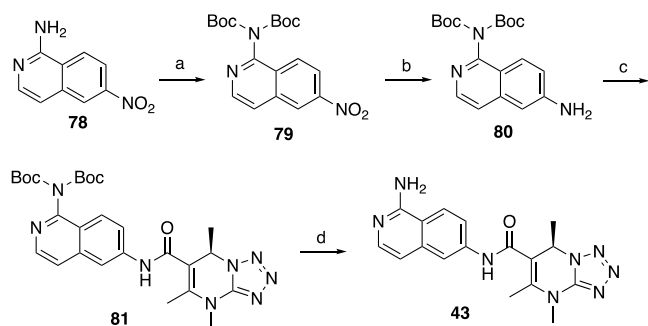
N-(1*H*-Indazol-5-yl)-4,5-dimethyl-4*H*,7*H*-[1,2,3,4]tetrazolo[1,5-*a*]pyrimidine-6-carboxamide (1). Carboxylic acid 49 (110 mg, 0.43 mmol) was dissolved in 3 mL of DMF. Et₃N (119 μL, 0.85 mmol), 1*H*-indazol-5-amine (113 mg, 0.85 mmol), and HATU (194 mg, 0.51 mmol) were added at 0 °C, and the reaction mixture was stirred at 0 °C for 2 h. The solvent was evaporated, and the residue was taken up in CH₃CN (1 mL with 0.1% formic acid) and then purified by reversed-phase column chromatography using a 2–10% CH₃CN/H₂O (0.1% formic acid) gradient eluent to give a purple solid (22 mg) of insufficient purity. The material was then further purified by

silica gel chromatography using a 0–10% MeOH/EtOAc gradient eluent to afford 1 as a pale pink solid (4.1 mg, 2%). ¹H NMR (400 MHz, DMSO-*d*₆) δ 12.99 (br s, 1H), 9.99 (s, 1H), 8.14 (s, 1H), 8.04 (s, 1H), 7.44–7.55 (m, 2H), 5.28 (s, 2H), 3.43 (s, 3H), 2.25 (s, 3H). MS-ESI (*m/z*) calcd for C₁₄H₁₅N₈O [M + H]⁺: 311.1. Found 311.0.

4,5-Dimethyl-*N*-(3-methyl-2*H*-indazol-5-yl)-4,7-dihydro-tetrazolo[1,5-*a*]pyrimidine-6-carboxamide (2). To a solution of carboxylic acid 49 in 2 mL of DCM were added (COCl)₂ (98 mg, 770 μmol) and one drop of DMF. The mixture was stirred at 25 °C for 30 min and concentrated to afford 4,5-dimethyl-4,7-dihydro-tetrazolo[1,5-*a*]pyrimidine-6-carboxamide as a yellow solid. Next, a solution of 3-methyl-1*H*-indazol-5-amine (70 mg, 475.62 μmol) in pyridine (1 mL) was cooled to 0 °C and then 4,5-

Scheme 9. Synthesis of Inhibitor 36^a

^aReagents: (a) MeMgBr, NaBH₄, THF, MeOH, 25 °C, 94%; (b) ethyl formate, AlMe₃, toluene, 90 °C, 10%; (c) POCl₃, toluene, 80 °C, 93%; (d) CDI, NH₃·H₂O, THF, 20 °C, 5%; and (e) Cs₂CO₃, Pd₂(dba)₃, Xantphos, dioxane, 90 °C, 2%.

Scheme 10. Synthesis of Inhibitor 43^a

^aReagents: (a) (Boc)₂O, 4-dimethylaminopyridine (DMAP), CH₃CN, 70 °C, 70%; (b) H₂, 10% Pd/C, EtOH, r.t., 97%; (c) (R)-32, EDCI, DMAP, pyridine, 70 °C, 93%; and (d) TFA, DCM, r.t., 51%.

dimethyl-4,7-dihydro-tetrazolo[1,5-*a*]pyrimidine-6-carboxyl chloride (122 mg, 571 μmol) in CH₃CN (0.2 mL) was added dropwise to the solution. The resulting mixture was stirred at 25 °C for 12 h. The reaction mixture was concentrated under reduced pressure to remove the solvent. The residue was purified by preparative HPLC (0.1% TFA) to afford 2 (36.9 mg, 17%) as a solid, pale yellow TFA salt. ¹H NMR (400 MHz, DMSO-*d*₆) δ 12.58 (br s, 1H), 9.95 (s, 1H), 8.08 (s, 1H), 7.46–7.38 (m, 2H), 5.28 (s, 2H), 3.43 (s, 3H), 2.45 (s, 3H), 2.25 (s, 3H). MS-ESI (*m/z*) calcd for C₁₅H₁₇N₈O [M + H]⁺: 325.1. Found 325.1.

4,5-Dimethyl-N-(3-(pyridin-4-yl)-1H-indazol-5-yl)-4,7-dihydro-tetrazolo[1,5-*a*]pyrimidine-6-carboxamide (3). To a solution of carboxylic acid 49 (100 mg, 512 μmol) in DCM (5 mL) was added T3P (50 wt % in EtOAc, 0.457 mL, 768 μmol) and Et₃N (156 mg, 1.54 mmol) followed by amine 46 (118 mg, 564 μmol). The reaction mixture was stirred at 15 °C for 12 h and concentrated. The mixture was purified by preparative HPLC (neutral) and further purified by additional preparative HPLC (0.1% TFA) to afford 3 (14 mg, 5%) as a light-yellow, solid TFA salt. ¹H NMR (400 MHz, DMSO-*d*₆) δ 13.99 (s, 1H), 10.16 (s, 1H), 8.88 (d, *J* = 6.0 Hz, 2H), 8.68 (s, 1H), 8.26 (d, *J* = 6.0 Hz, 2H), 7.59–7.76 (m, 2H), 5.32 (s, 2H), 3.46 (s, 3H), 2.29 (s, 3H). MS-ESI (*m/z*) calcd for C₁₉H₁₈N₉O [M + H]⁺: 388.2. Found: 388.1.

4,5-Dimethyl-N-(3-(2-morpholinopyridin-4-yl)-1H-indazol-5-yl)-4,7-dihydro-tetrazolo[1,5-*a*]pyrimidine-6-carboxamide (4). To a solution of carboxylic acid 49 (100 mg, 512 μmol) in DCM (3 mL) were added T3P (50 wt % in EtOAc, 424 mg, 666 μmol), Et₃N (156 mg, 1.54 mmol), and 3-(2-morpholinopyridin-4-yl)-1H-indazol-5-amine (182 mg, 615 μmol). The mixture was stirred at 15 °C for 12 h. The residue was purified by preparative HPLC to afford 4 (41 mg, 15%) as a white solid. ¹H NMR (400 MHz, DMSO-*d*₆) δ 13.44 (s, 1H), 10.06 (s, 1H), 8.52 (s, 1H), 8.28 (d, *J* = 5.1 Hz, 1H), 7.58–7.66

(m, 2H), 7.28 (s, 1H), 7.22 (d, *J* = 5.3 Hz, 1H), 5.30 (s, 2H), 3.72–3.77 (m, 4H), 3.50–3.55 (m, 4H), 3.44 (s, 3H), 2.27 (s, 3H). MS-ESI (*m/z*) calcd for C₂₃H₂₅N₁₀O₂ [M + H]⁺: 473.2. Found: 473.3.

4,5-Dimethyl-N-(3-(6-morpholinopyrimidin-4-yl)-1H-indazol-5-yl)-4,7-dihydro-tetrazolo[1,5-*a*]pyrimidine-6-carboxamide (5). A mixture of 3-(6-morpholinopyrimidin-4-yl)-1H-indazol-5-amine (150 mg, 507 μmol), carboxylic acid 49 (66 mg, 338 μmol), Et₃N (103 mg, 1.01 mmol, 141 μL), and T3P (50 wt % in EtOAc, 258 mg, 406 μmol, 241 μL) in DCM (2 mL) was degassed and purged with N₂ (3×); then, the mixture was stirred at 20 °C for 12 h under a N₂ atmosphere. The reaction mixture was concentrated under reduced pressure to remove the solvent. The residue was purified by preparative HPLC (0.1% TFA) to afford 5 (11 mg, 5%) as a solid, red TFA salt. ¹H NMR (400 MHz, DMSO-*d*₆) δ 13.81 (s, 1H), 10.12 (s, 1H), 8.74–8.69 (m, 2H), 7.74–7.68 (m, 1H), 7.66–7.60 (m, 1H), 7.44–7.40 (m, 1H), 5.30 (s, 2H), 3.76 (d, *J* = 8.6 Hz, 8H), 3.43 (s, 3H), 2.27 (s, 3H). MS-ESI (*m/z*) calcd for C₂₂H₂₃N₁₁O₂ [M + H]⁺: 474.2. Found 474.2.

4,5-Dimethyl-N-(3-(4-sulfamoylphenyl)-1H-indazol-5-yl)-4,7-dihydro-tetrazolo[1,5-*a*]pyrimidine-6-carboxamide (6). To a solution of bromoindazole 51 (50.0 mg, 128 μmol) and (4-sulfamoylphenyl)boronic acid (25.8 mg, 128 μmol) in 2 mL of DMF and 0.5 mL of H₂O were added tetrakis(triphenylphosphine)-palladium(0) (14.8 mg, 12.9 μmol) and Na₂CO₃ (41 mg, 385 μmol). The mixture was stirred at 100 °C for 12 h under a N₂ atmosphere. The reaction mixture was filtered, and the filtrate was concentrated to give a residue. The residue was purified by preparative HPLC (0.1% TFA) to afford 6 (12 mg, 16%) as a solid, white TFA salt. ¹H NMR (400 MHz, DMSO-*d*₆) δ 13.44 (s, 1H), 10.06 (s, 1H), 8.50 (s, 1H), 8.10 (m, *J* = 8.6 Hz, 2H), 7.97 (m, *J* = 8.6 Hz, 2H), 7.61 (s, 2H), 7.42 (s, 2H), 5.30 (s, 2H), 3.44 (s, 3H), 2.25–2.29 (m, 3H). MS-ESI (*m/z*) calcd for C₂₀H₂₀N₉O₃S [M + H]⁺: 466.1. Found: 466.1.

N-(3-(1H-Benzo[*d*]imidazol-2-yl)-1H-indazol-5-yl)-4,5-dimethyl-4,7-dihydro-tetrazolo[1,5-*a*]pyrimidine-6-carboxamide (7). To a solution of 3-(1H-benzo[*d*]imidazol-2-yl)-1H-indazol-5-amine (60.0 mg, 240.7 μmol) and carboxylic acid 49 (46.98 mg, 240.7 μmol) in pyridine (1 mL) was added EDCI (69.21 mg, 361.05 μmol). The reaction mixture was stirred at 30 °C for 12 h and then concentrated. The residue was purified by prep-HPLC (neutral) to afford the product (27.6 mg, 25%) as a pale yellow solid. ¹H NMR (400 MHz, DMSO-*d*₆) δ 13.75–13.47 (m, 1H), 13.11–12.85 (m, 1H), 10.15 (s, 1H), 8.76 (s, 1H), 7.82–7.46 (m, 4H), 7.27–7.17 (m, 2H), 5.33 (s, 2H), 3.44 (s, 3H), 2.29 (s, 3H). MS-ESI (*m/z*) calcd for C₂₁H₁₉N₁₀O [M + H]⁺: 427.2. Found 427.1.

N-(3-Bromo-1H-indazol-5-yl)-4,5-dimethyl-4,7-dihydro-tetrazolo[1,5-*a*]pyrimidine-6-carboxamide (8). To a solution of 3-bromo-1H-indazol-5-amine (30 mg, 141 μmol) and carboxylic acid 49 (28 mg, 141 μmol) in 2 mL of EtOAc were added T3P (50 wt % in EtOAc, 270 mg, 424 μmol, 252 μL) and Et₃N (57 mg, 565 μmol, 79 μL). The mixture was stirred at 60 °C for 12 h. The reaction mixture was then concentrated under reduced pressure to remove the solvent. The residue was purified by preparative HPLC (0.1% TFA) to afford 8 (9

mg, 15%) as a yellow, solid TFA salt. ^1H NMR (400 MHz, DMSO- d_6) δ 13.18–13.54 (m, 1H), 10.09 (s, 1H), 8.08 (s, 1H), 7.51–7.59 (m, 2H), 5.29 (s, 2H), 3.43 (s, 3H), 2.26 (s, 3H). MS-ESI (m/z) calcd for $\text{C}_{14}\text{H}_{14}\text{BrN}_3\text{O}$ [$\text{M} + \text{H}$] $^+$: 389.0. Found: 389.0.

N-(3-Carbamoyl-1*H*-indazol-5-yl)-4,5-dimethyl-4,7-dihydro-tetrazolo[1,5-*a*]pyrimidine-6-carboxamide (**9**). To a solution of 5-amino-1*H*-indazole-3-carboxamide (120 mg, 681 μmol) in DCM (4 mL) were added T3P (50 wt % in EtOAc, 650 mg, 1.02 mmol, 607 μL) and carboxylic acid **49** (133 mg, 681 μmol). The reaction mixture was stirred at 15 $^\circ\text{C}$ for 30 min and then Et_3N (344 mg, 3.41 mmol, 474 μL) was added, and the reaction mixture was stirred at 15 $^\circ\text{C}$ for 12 h. The reaction mixture was concentrated to give a residue, and the residue was purified by preparative HPLC (0.1% TFA) to afford **9** (23 mg, 7%) as a white, solid TFA salt. ^1H NMR (400 MHz, DMSO- d_6) δ 13.48 (s, 1H), 10.02 (s, 1H), 8.50 (s, 1H), 7.75–7.61 (m, 2H), 7.56 (d, $J = 8.8$ Hz, 1H), 7.32 (s, 1H), 5.29 (s, 2H), 3.43 (s, 3H), 2.26 (s, 3H). MS-ESI (m/z) calcd for $\text{C}_{15}\text{H}_{16}\text{N}_9\text{O}_2$ [$\text{M} + \text{H}$] $^+$: 354.13. Found 354.1.

N-(3-Benzamido-2*H*-indazol-5-yl)-4,5-dimethyl-4,7-dihydro-tetrazolo[1,5-*a*]pyrimidine-6-carboxamide (**10**). To a stirred solution of *N*-(5-amino-1*H*-indazol-3-yl)benzamide (100 mg, 396 μmol) and carboxylic acid **49** (77.4 mg, 396 μmol) in 2 mL of DCM were added T3P (50 wt % in EtOAc, 757 mg, 1.19 mmol, 707 μL) and Et_3N (160.45 mg, 1.59 mmol, 220.70 μL). The reaction mixture was then stirred at 25 $^\circ\text{C}$ for 12 h and concentrated. The residue was purified by preparative HPLC (neutral) to afford **10** (11.51 mg, 6%) as a colorless gum. ^1H NMR (400 MHz, DMSO- d_6) δ 9.97 (s, 1H) 7.94–8.09 (m, 3H) 7.43–7.62 (m, 5H) 5.24 (s, 2H) 3.39 (s, 3H) 2.21 (s, 3H). MS-ESI (m/z) calcd for $\text{C}_{21}\text{H}_{20}\text{N}_9\text{O}_2$ [$\text{M} + \text{H}$] $^+$: 430.2. Found 430.2.

N-(3-Butyramido-2*H*-indazol-5-yl)-4,5-dimethyl-4,7-dihydro-tetrazolo[1,5-*a*]pyrimidine-6-carboxamide (**11**). To a solution of *N*-(5-amino-1*H*-indazol-3-yl)butyramide (70 mg, 320 μmol) in 5 mL of DCM were added T3P (50 wt % in EtOAc, 408 mg, 641 μmol , 381 μL), carboxylic acid **49** (68.9 mg, 352 μmol), and Et_3N (97.4 mg, 962 μmol , 134 μL). The mixture was stirred at 40 $^\circ\text{C}$ for 12 h and concentrated. The residue was dissolved in DMF (2 mL) and purified by preparative HPLC (0.04% $\text{NH}_4\text{OH}/10$ mM NH_4HCO_3) to afford **11** (14.5 mg, 11%) as a yellow gum. ^1H NMR (400 MHz, DMSO- d_6) δ 12.60 (s, 1H), 10.22 (s, 1H), 9.97 (s, 1H), 7.99 (s, 1H), 7.55 (br d, $J = 8.68$ Hz, 1H) 7.40 (d, $J = 8.93$ Hz, 1H), 5.28 (s, 2H), 3.43 (s, 3H), 2.34–2.40 (m, 2H), 2.25 (s, 3H), 1.66 (sxt, $J = 7.29$ Hz, 2H), 0.97 (t, $J = 7.34$ Hz, 3H). MS-ESI (m/z) calcd for $\text{C}_{18}\text{H}_{22}\text{N}_9\text{O}_2$ [$\text{M} + \text{H}$] $^+$: 396.2. Found 396.1.

N-(1*H*-Indazol-5-yl)-4-methyl-4,7-dihydro-tetrazolo[1,5-*a*]pyrimidine-6-carboxamide (**12**). To a solution of 4-methyl-7*H*-tetrazolo[1,5-*a*]pyrimidine-6-carboxylic acid (90 mg, 496.82 μmol) and 1*H*-indazol-5-amine (66.15 mg, 496.82 μmol) in 2 mL of DMF were added DIEA (192.63 mg, 1.49 mmol, 259.61 μL), EDCI (142.86 mg, 745.23 μmol), and HOBt (100.70 mg, 745.23 μmol). The mixture was stirred at 15 $^\circ\text{C}$ for 15 h. The mixture was then purified by preparative HPLC to afford **12** (37.45 mg, 18%) as a gray, solid TFA salt. ^1H NMR (400 MHz, DMSO- d_6) δ 13.01 (br s, 1H), 9.63 (s, 1H), 8.09 (s, 1H), 8.03 (s, 1H), 7.60 (s, 1H), 7.50 (d, $J = 0.7$ Hz, 2H), 5.26 (s, 2H), 3.43 (s, 3H). MS-ESI (m/z) calcd for $\text{C}_{13}\text{H}_{13}\text{N}_8\text{O}$ [$\text{M} + \text{H}$] $^+$: 297.1. Found 297.1.

5-Ethyl-*N*-(1*H*-indazol-5-yl)-4-methyl-4*H*,7*H*-[1,2,3,4]tetrazolo[1,5-*a*]pyrimidine-6-carboxamide (**13**). A solution of 5-ethyl-4-methyl-4,7-dihydro-tetrazolo[1,5-*a*]pyrimidine-6-carboxylic acid (34 mg, 0.16 mmol) and 1*H*-indazol-5-amine (43 mg, 0.32 mmol) in 1.5 mL of anhydrous DMF was stirred at 0 $^\circ\text{C}$. HATU (74 mg, 0.2 mmol) was then added followed by Et_3N (45 μL , 0.32 mmol). The reaction mixture was stirred for 30 min at 0 $^\circ\text{C}$ and concentrated to give a residue. The residue was taken up in CH_3CN (with 0.1% TFA) and purified by reversed-phase chromatography using a 2–10% $\text{CH}_3\text{CN}/\text{H}_2\text{O}$ (0.1% formic acid) gradient eluent to afford **13** as a red solid of insufficient purity. The compound was then repurified on silica gel using a 0–20% MeOH/EtOAc gradient eluent to give **13** (32 mg, 62%) as a white solid. ^1H NMR (400 MHz, DMSO- d_6) δ 13.00 (br s, 1H), 9.97 (s, 1H), 8.15 (s, 1H), 8.04 (s, 1H), 7.33–7.70

(m, 2H), 5.31 (s, 2H), 3.43 (s, 3H), 2.63 (q, $J = 7.60$ Hz, 2H), 1.17 (t, $J = 7.45$ Hz, 3H). MS-ESI (m/z) calcd for $\text{C}_{15}\text{H}_{17}\text{N}_8\text{O}$ [$\text{M} + \text{H}$] $^+$: 325.1. Found 325.3.

4-Ethyl-*N*-(1*H*-indazol-5-yl)-5-methyl-4,7-dihydro-tetrazolo[1,5-*a*]pyrimidine-6-carboxamide (**14**). Ethyl 4-ethyl-5-methyl-4,7-dihydro-tetrazolo[1,5-*a*]pyrimidine-6-carboxylate (136 mg, 0.573 mmol) and 1*H*-indazol-5-amine (153 mg, 1.15 mmol) were added to anhydrous DMF (1.5 mL) at 0 $^\circ\text{C}$, and HATU (262 mg, 0.688 mmol) and Et_3N (160 μL , 1.15 mmol) were added. The mixture was stirred for 3 h and then allowed to warm to r.t. The temperature was then increased to 40 $^\circ\text{C}$, and another portion of HATU (131 mg) and 1*H*-indazol-5-amine (76.5 mg) was added. The reaction was then stirred at 40 $^\circ\text{C}$ for an additional 3 h. Water was added, and the mixture was extracted with EtOAc. The combined organic phases were concentrated, and the residue was triturated with water and then with MeOH to afford **14** (53 mg, 29%) as a pale purple solid. ^1H NMR (400 MHz, DMSO- d_6) δ 13.00 (br s, 1H), 10.00 (br s, 1H), 8.15 (br s, 1H), 8.05 (s, 1H), 7.50 (br s, 2H), 5.28 (br s, 2H), 3.92 (d, $J = 7.26$ Hz, 2H), 2.26 (s, 3H), 1.24 (t, $J = 6.93$ Hz, 3H). MS-ESI (m/z) calcd for $\text{C}_{15}\text{H}_{17}\text{N}_8\text{O}$ [$\text{M} + \text{H}$] $^+$: 325.2. Found 325.3.

N-(1*H*-Indazol-5-yl)-5-methyl-4-[2-(morpholin-4-yl)ethyl]-4*H*,7*H*-[1,2,3,4]tetrazolo[1,5-*a*]pyrimidine-6-carboxamide (**15**). 5-Methyl-4-(2-morpholinoethyl)-4,7-dihydro-tetrazolo[1,5-*a*]pyrimidine-6-carboxylic acid (40 mg, 0.12 mmol) was dissolved in 1.5 mL of DMF. Et_3N (32 μL , 0.23 mmol), 1*H*-indazol-5-amine (18 mg, 0.14 mmol), and HATU (52 mg, 0.14 mmol) were added at 0 $^\circ\text{C}$, and the reaction mixture was stirred for 3 h. The temperature was brought to 40 $^\circ\text{C}$, and additional HATU (52 mg, 0.14 mmol) and 1*H*-indazol-5-amine (18 mg, 0.14 mmol) were added. Stirring at 40 $^\circ\text{C}$ was continued for 3 h. H_2O (15 mL) was added followed by EtOAc (15 mL). The organic layer was separated, concentrated, and the residue was purified by reversed-phase chromatography using a 0–10% MeOH/EtOAc gradient eluent to give a solid, which was further purified on reversed-phase preparative TLC using the same gradient to afford **15** (4.5 mg, 10%) as a white solid. ^1H NMR (400 MHz, DMSO- d_6) δ 12.91 (br s, 1H), 10.02 (br s, 1H), 8.14 (s, 1H), 8.04 (s, 1H), 7.41–7.57 (m, 2H), 5.27 (s, 2H), 3.97 (t, $J = 6.7$ Hz, 2H), 3.52 (t, $J = 4.4$ Hz, 4H), 2.56 (t, $J = 6.7$ Hz, 2H), 2.41–2.48 (m, 4H), 2.26 (s, 3H). MS-ESI (m/z) calcd for $\text{C}_{19}\text{H}_{23}\text{N}_9\text{O}_2$ [$\text{M} + \text{H}$] $^+$: 410.2. Found 410.3.

N 6 -(1*H*-Indazol-5-yl)-*N* 4 ,*N* 5 -5-trimethyltetrazolo[1,5-*a*]pyrimidine-4,6(7*H*)-dicarboxamide (**16**). To a solution of 4-(dimethylcarbamoyl)-5-methyl-4,7-dihydro-tetrazolo[1,5-*a*]pyrimidine-6-carboxylic acid (85.0 mg, 337 μmol) and 1*H*-indazol-5-amine (45.0 mg, 337 μmol) in DCM (5 mL) were added T3P (50 wt % in EtOAc, 322 mg, 506 μmol , 301 μL) and Et_3N (102 mg, 1.01 mmol, 141 μL). The mixture was stirred at 15 $^\circ\text{C}$ for 2 h and concentrated to give a residue. The residue was purified by preparative HPLC (with 0.1% TFA) to afford **16** (38 mg, 23%) as a light pink, solid TFA salt. ^1H NMR (400 MHz, CD_3OD) δ 8.14 (s, 1H), 8.05 (s, 1H), 7.58–7.49 (m, 2H), 5.32 (s, 2H), 3.17 (s, 3H), 3.14 (s, 3H), 2.24 (s, 3H). MS-ESI (m/z) calcd for $\text{C}_{16}\text{H}_{18}\text{N}_9\text{O}_2$ [$\text{M} + \text{H}$] $^+$: 368.15. Found: 368.2.

N-(1*H*-Indazol-5-yl)-5-methyl-4-phenyl-4,7-dihydro-tetrazolo[1,5-*a*]pyrimidine-6-carboxamide (**17**). To a solution of 5-methyl-4-phenyl-4,7-dihydro-tetrazolo[1,5-*a*]pyrimidine-6-carboxylic acid (130 mg, 505 μmol) and 1*H*-indazol-5-amine (81 mg, 606 μmol) in EtOAc (2 mL) were added T3P (50 wt % in EtOAc, 965 mg, 1.52 mmol) and Et_3N (204 mg, 2.02 mmol). The mixture was stirred at 60 $^\circ\text{C}$ for 12 h and concentrated to give a residue. The residue was purified by preparative HPLC (with 0.1% TFA) to afford **17** (31 mg, 16%) as a red, gummy TFA salt. ^1H NMR (400 MHz, DMSO- d_6) δ 10.07 (s, 1H), 8.16 (s, 1H), 8.05 (s, 1H), 7.43–7.61 (m, 7H) 5.41 (s, 2H), 1.88 (s, 3H). MS-ESI (m/z) calcd for $\text{C}_{19}\text{H}_{18}\text{N}_8\text{O}$ [$\text{M} + \text{H}$] $^+$: 373.14. Found: 373.1.

4-Acetyl-*N*-(1*H*-indazol-5-yl)-5-methyl-4,7-dihydro-tetrazolo[1,5-*a*]pyrimidine-6-carboxamide (**18**). To a solution of *N*-(2*H*-indazol-5-yl)-5-methyl-4,7-dihydro-tetrazolo[1,5-*a*]pyrimidine-6-carboxamide (50 mg, 169 μmol) and Et_3N (34.2 mg, 337 μmol , 47.0 μL) in DCM (6 mL) was added acetyl chloride (19.9 mg, 253 μmol , 18.1 μL) at 15 $^\circ\text{C}$ and the reaction mixture was stirred for 0.5 h. The reaction

mixture was concentrated under reduced pressure to give a residue. The residue was purified by preparative HPLC to give **18** (4.1 mg, 6%) as a gummy, yellow TFA salt. $^1\text{H NMR}$ (400 MHz, $\text{DMSO-}d_6$) δ 13.01 (br s, 1H), 10.41 (s, 1H), 8.18 (s, 1H), 8.06 (s, 1H), 7.55–7.46 (m, 2H), 5.22 (d, $J = 1.3$ Hz, 2H), 2.59 (s, 3H), 2.33–2.30 (m, 3H). MS-ESI (m/z) calcd for $\text{C}_{15}\text{H}_{15}\text{N}_8\text{O}_2$ [$\text{M} + \text{H}$] $^+$: 339.1. Found 339.1.

N-(1*H*-Indazol-5-yl)-*N*,4,5-trimethyl-4,7-dihydro-tetrazolo[1,5-*a*]pyrimidine-6-carboxamide (**19**). Carboxylic acid **49** (70 mg, 0.36 mmol) and *N*-methyl-1*H*-indazol-5-amine (**56**) (79 mg, 0.54 mmol) were dissolved in anhydrous DMF (2 mL). Then, the solution was cooled to 0 °C with an ice–water bath and Et_3N (0.1 mL, 0.72 mmol) and HATU (164 mg, 0.43 mmol) were added. The mixture was stirred at 0 °C for 30 min and then at r.t. overnight. The solution was loaded directly on a C18 column and purified by reversed-phase chromatography using a 5–30% $\text{CH}_3\text{CN}/\text{H}_2\text{O}$ (0.1% formic acid) gradient eluent. The purest fractions were combined, evaporated under reduced pressure, and subjected to an additional purification by silica gel chromatography using a 0–20% MeOH/EtOAc gradient eluent to afford **19** (25 mg, 21%) as a white solid. $^1\text{H NMR}$ (400 MHz, $\text{DMSO-}d_6$) δ 13.15 (br s, 1H), 8.06 (s, 1H), 7.77 (d, $J = 1.54$ Hz, 1H), 7.52 (d, $J = 8.80$ Hz, 1H), 7.34 (dd, $J = 8.80, 1.98$ Hz, 1H), 4.94 (br s, 2H), 3.31 (s, 3H), 3.19 (s, 3H), 1.96 (s, 3H). MS-ESI (m/z) calcd for $\text{C}_{15}\text{H}_{17}\text{N}_8\text{O}$ [$\text{M} + \text{H}$] $^+$: 325.2. Found 325.2.

N-(1*H*-Indazol-5-yl)-4,5-dimethyl-4,7-dihydro-tetrazolo[1,5-*a*]pyrimidine-6-carbothioamide (**20**). Lawesson's reagent (782 mg, 1.93 mmol) was added to a solution of compound **1** (300 mg, 0.95 mmol) in 8 mL of anhydrous dioxane. The solution was stirred at 100 °C for 2 h. Additional Lawesson's reagent (782 mg, 1.93 mmol) was added, and stirring was continued at 100 °C for 18 h. The solvent was removed to afford the crude product that was purified by preparative HPLC to afford 108 mg of **20**, which was insufficiently pure (~80%). Thirty milligrams of this material was taken up in DMSO and further purified by reversed-phase chromatography using a 0–50% $\text{CH}_3\text{CN}/\text{H}_2\text{O}$ (0.1% formic acid) gradient as eluent to give **20** (10 mg, 3%) as a yellow solid. $^1\text{H NMR}$ (400 MHz, $\text{DMSO-}d_6$) δ 13.17 (br s, 1H), 11.80 (s, 1H), 8.38 (s, 1H), 8.13 (s, 1H), 7.49–7.66 (m, 2H), 5.30 (s, 2H), 3.45 (s, 3H), 2.18 (s, 3H). MS-ESI (m/z) calcd for $\text{C}_{14}\text{H}_{15}\text{N}_8\text{O}$ [$\text{M} + \text{H}$] $^+$: 327.1. Found 327.2.

rac-N-(1*H*-Indazol-5-yl)-4,5,7-trimethyl-4,7-dihydro-tetrazolo[1,5-*a*]pyrimidine-6-carboxamide (**21** and **22**). A solution of compound **32** (70 mg, 0.34 mmol) and 1*H*-indazol-5-amine (89 mg, 0.67 mmol) in 2 mL of anhydrous DMF was stirred at 0 °C, and HATU (153 mg, 0.402 mmol) was added followed by Et_3N (94 μL , 0.67 mmol). The resulting mixture was then stirred for 2 h at r.t. Water (15 mL) was added, and the mixture was extracted with EtOAc (15 mL). The organic layer was concentrated, and the residue was purified by reversed-phase chromatography using a 2–10% $\text{CH}_3\text{CN}/\text{H}_2\text{O}$ (0.1% formic acid) gradient eluent to give a solid, which was triturated with MeOH to afford a racemic mixture of compounds **21** and **22** (21 mg, 19%) as a pale purple solid.

The enantiomers were then separated using semipreparative chiral HPLC (column: Whelk O1 (R,R) (25 cm \times 2.0 cm), 10 μm ; mobile phase: *n*-hexane/ EtOH 40/60% v/v; flow rate: 17 mL/min. DAD detection: 220 nm; loop: 3000 μL). Solubilization: 13 mg in 3 mL of 1:1 hexafluoro-2-propanol/ EtOH .

(*R*)-*N*-(1*H*-Indazol-5-yl)-4,5,7-trimethyl-4,7-dihydro-tetrazolo[1,5-*a*]pyrimidine-6-carboxamide (**21**). Second eluting enantiomer. $^1\text{H NMR}$ (400 MHz, $\text{DMSO-}d_6$) δ 12.99 (br s, 1H), 10.17 (br s, 1H), 8.16 (s, 1H), 8.05 (s, 1H), 7.29–7.63 (m, 2H), 5.74 (d, $J = 6.38$ Hz, 1H), 3.43 (s, 3H), 2.19 (s, 3H), 1.57 (d, $J = 6.16$ Hz, 3H). MS-ESI (m/z) calcd for $\text{C}_{15}\text{H}_{17}\text{N}_8\text{O}$ [$\text{M} + \text{H}$] $^+$: 325.1. Found 325.2.

(*S*)-*N*-(1*H*-Indazol-5-yl)-4,5,7-trimethyl-4,7-dihydro-tetrazolo[1,5-*a*]pyrimidine-6-carboxamide (**22**). First eluting enantiomer. $^1\text{H NMR}$ (400 MHz, $\text{DMSO-}d_6$) δ 12.99 (br s, 1H), 10.17 (s, 1H), 8.16 (s, 1H), 8.05 (d, $J = 0.75$ Hz, 1H), 7.43–7.57 (m, 2H), 5.74 (q, $J = 6.02$ Hz, 1H), 3.43 (s, 3H), 2.19 (d, $J = 1.00$ Hz, 3H), 1.57 (d, $J = 6.53$ Hz, 3H). MS-ESI (m/z) calcd for $\text{C}_{15}\text{H}_{17}\text{N}_8\text{O}$ [$\text{M} + \text{H}$] $^+$: 325.1. Found 325.2.

(*R*)-4,5,7-Trimethyl-*N*-(3-methyl-1*H*-indazol-5-yl)-4,7-dihydro-tetrazolo[1,5-*a*]pyrimidine-6-carboxamide (**23**). Carboxylic

acid (**R**)-**32** (35 mg, 0.17 mmol) and 3-methyl-1*H*-indazol-5-amine (48 mg, 0.33 mmol) were dissolved in 2 mL of anhydrous DMF. The solution was then cooled to 0 °C in an ice–water bath, and Et_3N (0.05 mL, 0.33 mmol) and HATU (76 mg, 0.20 mmol) were added. The reaction mixture was stirred at 0 °C for 5 min and then at r.t. for 6 h. The material was purified by reversed-phase chromatography using a 5–25% $\text{CH}_3\text{CN}/\text{H}_2\text{O}$ (0.1% formic acid) gradient eluent. Product-containing fractions were combined and further purified by silica gel column chromatography using a 0–10% MeOH/EtOAc gradient eluent to afford **23** (33 mg, 57%) as a white solid. $^1\text{H NMR}$ (400 MHz, $\text{DMSO-}d_6$) δ 12.58 (s, 1H), 10.15 (s, 1H), 8.11 (s, 1H), 7.43 (s, 2H), 5.74 (d, $J = 6.16$ Hz, 1H), 3.43 (s, 3H), 2.47 (s, 3H), 2.20 (d, $J = 0.88$ Hz, 3H), 1.57 (d, $J = 6.38$ Hz, 3H). MS-ESI (m/z) calcd for $\text{C}_{16}\text{H}_{19}\text{N}_8\text{O}$ [$\text{M} + \text{H}$] $^+$: 339.3. Found 339.2.

(*S*)-4,5,7-Trimethyl-*N*-(3-methyl-1*H*-indazol-5-yl)-4,7-dihydro-tetrazolo[1,5-*a*]pyrimidine-6-carboxamide (**24**). To a stirred solution of methyl 4,5,7-trimethyl-7*H*-tetrazolo[1,5-*a*]pyrimidine-6-carboxylate (25 g, 112 mmol) in 1 L of toluene were added 3-methyl-1*H*-indazol-5-amine (14.67 g, 99.67 mmol) and AlMe_3 (2 M, 112 mL). The reaction mixture was then stirred at 120 °C for 12 h. After cooling to 0 °C, the reaction mixture was quenched with saturated aqueous potassium sodium tartrate (1 L) and filtered. The solid obtained was washed with water (2 L) and petroleum ether (2 L) and then concentrated. This process was repeated an additional 3 \times , and material from all four batches was combined and purified by silica gel chromatography using a 0.5–1.7% MeOH/DCM gradient eluent to give the racemic product (60 g, 40%) as an off-white solid. Thirty grams of the solid was dissolved in a mixture of MeOH (1 L), CH_3CN (2 L), *i*-PrOH (3 L), and CHCl_3 (0.5 L) and stirred at 20 °C for 0.5 h. The mixture was separated by SFC to give **24** (14 g, 46%) as an off-white solid. $^1\text{H NMR}$ (400 MHz, $\text{DMSO-}d_6$) δ 12.58 (s, 1H), 10.15 (s, 1H), 8.10 (s, 1H), 7.42 (s, 2H), 5.73 (q, $J = 6.0$ Hz, 1H), 3.42 (s, 3H), 2.47–2.43 (m, 3H), 2.19 (s, 3H), 1.56 (d, $J = 6.4$ Hz, 3H). MS-ESI (m/z) calcd for $\text{C}_{16}\text{H}_{19}\text{N}_8\text{O}$ [$\text{M} + \text{H}$] $^+$: 339.1. Found 339.2.

(*R*)-4,5,7-Trimethyl-*N*-(3-(pyridin-4-yl)-1*H*-indazol-5-yl)-4,7-dihydro-tetrazolo[1,5-*a*]pyrimidine-6-carboxamide (**25**). (*R*)-*N*-(3-Bromo-1*H*-indazol-5-yl)-4,5,7-trimethyl-4,7-dihydro-tetrazolo[1,5-*a*]pyrimidine-6-carboxamide (50 mg, 0.12 mmol), (pyridin-4-yl)boronic acid (31 mg, 0.25 mmol), and Na_2CO_3 (39 mg, 0.37 mmol) were suspended in 2 mL of DMF and 0.5 mL of water. The mixture was purged with N_2 for 5 min, and then $\text{Pd}(\text{PPh}_3)_4$ (7 mg, 0.006 mmol) was added. The reaction mixture was stirred at 100 °C for 6 h under N_2 , and then it was irradiated using a microwave at 100 °C for 30 min. The mixture was partitioned between water and EtOAc ; the phases were separated, and the aqueous layer was extracted with EtOAc . The combined organic layers were washed with water, dried over anhydrous Na_2SO_4 , and the solvent was removed under reduced pressure. The material was purified by silica gel chromatography eluting with a 0–100% $\text{EtOAc}/\text{cyclohexane}$ gradient followed by a 0–10% MeOH/EtOAc gradient to afford **25** of insufficient purity. The material was then further purified by reversed-phase chromatography using a 0–25% $\text{CH}_3\text{CN}/\text{H}_2\text{O}$ (0.1% formic acid) gradient eluent to afford **25** (5 mg, 10%) as a yellow solid. $^1\text{H NMR}$ (400 MHz, $\text{DMSO-}d_6$) δ 13.58 (br s, 1H), 10.30 (s, 1H), 8.67–8.78 (m, 2H), 8.59 (s, 1H), 7.87–7.97 (m, 2H), 7.64 (s, 2H), 5.62–5.95 (m, 1H), 3.45 (s, 3H), 2.22 (s, 3H), 1.58 (d, $J = 6.38$ Hz, 3H). MS-ESI (m/z) calcd for $\text{C}_{20}\text{H}_{20}\text{N}_9\text{O}$ [$\text{M} + \text{H}$] $^+$: 402.2. Found 402.2.

rac-4,5,7-Trimethyl-*N*-(3-(2-morpholinopyridin-4-yl)-1*H*-indazol-5-yl)-4,7-dihydro-tetrazolo[1,5-*a*]pyrimidine-6-carboxamide (**26** and **27**). To a solution of carboxamide **61** (35 mg, 0.06 mmol) in 2 mL of THF was added 0.5 mL of 4 M HCl in dioxane. The reaction mixture was stirred at r.t. for 1 h. At this point, reaction monitoring indicated degradation of the starting material in addition to the formation of the desired product. The reaction mixture was quenched with water and extracted with EtOAc . The combined organic layers were washed with water, dried over Na_2SO_4 , and evaporated to dryness. The residue was redissolved in THF (2 mL) and tetra-*n*-butylammonium fluoride (TBAF, 1 M in THF, 1 mL). The reaction mixture was stirred at r.t. over the weekend and then at 70 °C for 3 h.

After cooling to r.t., the mixture was diluted with EtOAc, washed with water, and concentrated. The material was purified by reversed-phase column chromatography using a 5–25% CH₃CN/H₂O (0.1% formic acid) gradient eluent to afford a racemic mixture of **26** and **27** (5 mg, 18%).

The enantiomers were then separated using chiral HPLC (column: Chiralpak AD-H (25 cm × 2.0 cm), 5 μm; mobile phase: *n*-hexane/EtOH/MeOH 70/15/15% v/v; flow rate: 18 mL/min. DAD detection: 220 nm; loop: 500 μL). Solubilization: 3 mg in 1 mL of EtOH.

(*R*)-4,5,7-Trimethyl-*N*-(3-(2-morpholinopyridin-4-yl)-1*H*-indazol-5-yl)-4,7-dihydro-tetrazolo[1,5-*a*]pyrimidine-6-carboxamide (**26**). Second eluting enantiomer. ¹H NMR (400 MHz, MeOD) δ 8.57 (s, 1H), 8.27 (d, *J* = 5.28 Hz, 1H), 7.55–7.66 (m, 2H), 7.39 (s, 1H), 7.31–7.36 (m, 1H), 5.76 (q, *J* = 6.24 Hz, 1H), 3.82–3.93 (m, 4H), 3.57–3.65 (m, 4H), 3.52 (s, 3H), 2.30 (d, *J* = 1.10 Hz, 3H), 1.70 (d, *J* = 6.38 Hz, 3H). MS-ESI (*m/z*) calcd for C₂₄H₂₇N₁₀O₂ [M + H]⁺: 487.2. Found 487.8.

(*S*)-4,5,7-Trimethyl-*N*-(3-(2-morpholinopyridin-4-yl)-1*H*-indazol-5-yl)-4,7-dihydro-tetrazolo[1,5-*a*]pyrimidine-6-carboxamide (**27**). First eluting enantiomer. ¹H NMR (400 MHz, MeOD) δ 8.57 (s, 1H), 8.27 (d, *J* = 5.28 Hz, 1H), 7.55–7.66 (m, 2H), 7.39 (s, 1H), 7.31–7.36 (m, 1H), 5.76 (q, *J* = 6.24 Hz, 1H), 3.82–3.93 (m, 4H), 3.57–3.65 (m, 4H), 3.52 (s, 3H), 2.30 (d, *J* = 1.10 Hz, 3H), 1.70 (d, *J* = 6.38 Hz, 3H). MS-ESI (*m/z*) calcd for C₂₄H₂₇N₁₀O₂ [M + H]⁺: 487.2. Found 487.8.

N-(1*H*-Indazol-5-yl)-4,5,7,7-tetramethyl-4*H*,7*H*-[1,2,3,4]-tetrazolo[1,5-*a*]pyrimidine-6-carboxamide (**28**). Carboxamide **67** (7.5 mg, 0.017 mmol) was dissolved in 2 mL of DCM. TFA (0.5 mL) was added dropwise at 0 °C, and the reaction mixture was stirred at r.t. for 3 h. The solvent was evaporated under reduced pressure, and the material was purified by preparative HPLC to afford **28** (2.1 mg, 4%, three steps) as a white solid. ¹H NMR (400 MHz, DMSO-*d*₆) δ 8.15 (d, *J* = 1.10 Hz, 1H), 8.06 (s, 1H), 7.47–7.63 (m, 2H), 3.46–3.54 (m, 3H), 2.23 (s, 3H), 1.90 (s, 6H). MS-ESI (*m/z*) calcd for C₁₆H₁₉N₈O [M + H]⁺: 339.2. Found 339.8.

4,5,7,7-Tetramethyl-*N*-(3-methyl-2*H*-indazol-5-yl)-4,7-dihydro-tetrazolo[1,5-*a*]pyrimidine-6-carboxamide (**29**). To a solution of methyl ester **65** (50 mg, 339 μmol) and 3-methyl-1*H*-indazol-5-amine (100 mg, 421 μmol) in 2 mL of toluene was added Al(CH₃)₃ (2 M in toluene, 679.45 μL), and the mixture was stirred at 90 °C for 12 h. The reaction was quenched with MeOH (2 mL), and then the mixture was concentrated. The residue was purified by preparative HPLC to afford **29** (20 mg, 16%) as a pale yellow solid. ¹H NMR (400 MHz, DMSO-*d*₆) δ 8.08 (s, 1H) 7.46 (s, 2H) 3.49 (s, 3H) 2.55 (s, 3H) 2.22 (s, 3H) 1.88 (s, 6H). MS-ESI (*m/z*) calcd for C₁₇H₂₁N₈O [M + H]⁺: 353.2. Found 353.2.

4,5,7,7-Tetramethyl-*N*-(3-(2-morpholinopyridin-4-yl)-1*H*-indazol-5-yl)-4,7-dihydro-tetrazolo[1,5-*a*]pyrimidine-6-carboxamide (**30**). Carboxylic acid **66** (210 mg, 21% pure by NMR, 0.31 mmol theoretical) and 3-(2-morpholinopyridin-4-yl)-1*H*-indazol-5-amine (109 mg, 0.37 mmol) were dissolved in 2.5 mL of anhydrous DMF. The solution was cooled to 0 °C with an ice–water bath, and Et₃N (87 μL, 0.62 mmol) and HATU (143 mg, 0.38 mmol) were sequentially added. The mixture was stirred at 0 °C for 5 min and then at r.t. for 18 h. The mixture was partitioned between EtOAc and water and extracted. The combined organic layers were dried over Na₂SO₄, filtered, and concentrated. The material was purified by column chromatography (silica gel 110 NH₂) using a 0–10% MeOH/EtOAc gradient eluent to afford material of insufficient purity. The material was then further purified by chiral semipreparative HPLC (Chiralcel OD-H column; 25 cm × 2.0 cm) to afford **30** (10 mg, 7%) as a white solid. ¹H NMR (400 MHz, DMSO-*d*₆) δ 13.45 (br s, 1H), 10.34 (s, 1H), 8.56 (s, 1H), 8.30 (d, *J* = 5.06 Hz, 1H), 7.61 (d, *J* = 1.10 Hz, 2H), 7.29 (s, 1H), 7.23 (dd, *J* = 5.28, 1.10 Hz, 1H), 3.68–3.82 (m, 4H), 3.50–3.61 (m, 4H), 3.45 (s, 3H), 2.14 (s, 3H), 1.79 (s, 6H). MS-ESI (*m/z*) calcd for C₂₅H₂₉N₁₀O₂ [M + H]⁺: 501.2. Found 501.3.

4,5,7,7-Tetramethyl-*N*-(3-phenyl-1*H*-indazol-5-yl)-4,7-dihydro-tetrazolo[1,5-*a*]pyrimidine-6-carboxamide (**31**). To a sol-

ution of ester **65** (70 mg, 0.3 mmol) and 3-phenyl-1*H*-indazol-5-amine (93 mg, 0.44 mmol) in anhydrous toluene (3 mL) was added Al(CH₃)₃ (2 M in toluene, 0.44 mL, 0.89 mmol). The reaction mixture was stirred for 18 h at 90 °C. The reaction was cooled to r.t., quenched with water, and extracted with DCM. The organic phase was passed through a phase separator and concentrated under reduced pressure. The crude material was purified by reversed-phase column chromatography using a 5–50% CH₃CN/H₂O (0.1% formic acid) gradient eluent to afford material of insufficient purity. The material was then further purified by chiral semipreparative HPLC (Chiralcel OD-H column; 25 cm × 2.0 cm) to afford **30** (11 mg, 9%) as a white solid. ¹H NMR (400 MHz, DMSO-*d*₆) δ 13.22 (br s, 1H), 10.32 (s, 1H), 8.51 (s, 1H), 7.93 (d, *J* = 7.26 Hz, 2H), 7.52–7.63 (m, 4H), 7.38–7.47 (m, 1H), 3.44 (s, 3H), 2.14 (s, 3H), 1.79 (s, 6H). MS-ESI (*m/z*) calcd for C₂₂H₂₃N₈O [M + H]⁺: 415.2. Found 415.2.

4,5-Dimethyl-*N*-(3-methyl-1*H*-indol-5-yl)-4,7-dihydro-tetrazolo[1,5-*a*]pyrimidine-6-carboxamide (**33**). To a solution of 3-methyl-1*H*-indol-5-amine (90 mg, 615 μmol) and carboxylic acid **49** (120 mg, 615 μmol) in 2 mL of pyridine was added EDCI (177 mg, 923 μmol). The mixture was stirred at 25 °C for 4 h and concentrated. The residue was purified by preparative HPLC to afford **33** (12 mg, 6%) as a pale pink solid. ¹H NMR (400 MHz, DMSO-*d*₆) δ 10.68 (br s, 1H) 9.79 (s, 1H) 7.84 (s, 1H) 7.21–7.30 (m, 2H) 7.10 (s, 1H) 5.27 (s, 2H) 3.43 (s, 3H) 2.25 (s, 3H) 2.23 (s, 3H). MS-ESI (*m/z*) calcd for C₁₆H₁₈N₇O [M + H]⁺: 324.1. Found 324.1.

N-(1*H*-Benzo[*d*]imidazol-5-yl)-4,5-dimethyl-4,7-dihydro-tetrazolo[1,5-*a*]pyrimidine-6-carboxamide (**34**). Carboxylic acid **49** (70 mg, 0.36 mmol) and 1*H*-benzo[*d*]imidazol-5-amine (96 mg, 0.72 mmol) were dissolved in anhydrous DMF (2 mL). Then, the solution was cooled to 0 °C with an ice–water bath and Et₃N (0.10 mL, 0.72 mmol) and HATU (164 mg, 0.43 mmol) were added. The mixture was stirred at 0 °C for 30 min and then at r.t. overnight. The mixture was then diluted with water and concentrated under reduced pressure to remove some of the DMF before purifying the material by reversed-phase chromatography using a 2–15% CH₃CN/H₂O (0.1% formic acid) gradient eluent. Product-containing fractions were combined, evaporated to dryness, and subjected to an additional purification by reversed-phase chromatography using a 2–25% CH₃CN/H₂O (0.1% ammonium hydroxide) gradient eluent to afford **34** (20 mg, 18%). ¹H NMR (400 MHz, DMSO-*d*₆) δ 9.77 (br s, 1H) 8.20 (s, 1H) 8.02 (s, 1H) 7.53 (d, *J* = 8.60 Hz, 1H) 7.31–7.41 (m, 1H) 5.25 (s, 2H) 3.43 (s, 3H) 2.25 (d, *J* = 1.32 Hz, 3H). MS-ESI (*m/z*) calcd for C₁₄H₁₃N₈O [M + H]⁺: 311.1. Found 311.0.

4,5-Dimethyl-*N*-(3-methylimidazo[1,5-*a*]pyridin-6-yl)-4,7-dihydro-tetrazolo[1,5-*a*]pyrimidine-6-carboxamide (**35**). To a solution of carboxylic acid **49** (65 mg, 333 μmol) in 4 mL of DMF were added amine **72** (49.0 mg, 333 μmol) and *i*-Pr₂NEt (129 mg, 999 μmol). A solution of HATU (190 mg, 499 μmol) in 1 mL of DMF was then added to the mixture dropwise at 0 °C. The mixture was stirred at 0 °C for 1 h and then at 25 °C for 11 h. The reaction mixture was concentrated and purified by preparative HPLC (neutral condition) to afford **35** (21 mg, 16%, two steps) as a gray solid. ¹H NMR (400 MHz, DMSO-*d*₆) δ 9.95 (s, 1H) 8.71 (s, 1H) 7.51 (d, *J* = 10 Hz, 1H) 7.23 (s, 1H) 6.74–6.78 (m, 1H) 5.27 (s, 2H) 3.43 (s, 3H) 2.53 (s, 3H) 2.25 (s, 3H). MS-ESI (*m/z*) calcd for C₁₃H₁₇N₈O [M + H]⁺: 325.1. Found 325.0.

4,5-Dimethyl-*N*-(1-methylimidazo[1,5-*a*]pyridin-7-yl)-4,7-dihydro-tetrazolo[1,5-*a*]pyrimidine-6-carboxamide (**36**). To a solution of 4,5-dimethyl-7*H*-tetrazolo[1,5-*a*]pyrimidine-6-carboxamide (**77**) (10 mg, 52 μmol) and 7-bromo-1-methyl-imidazo[1,5-*a*]pyridine (**76**) (10.9 mg, 51.5 μmol) in 2 mL of dioxane were added Cs₂CO₃ (33.6 mg, 103 μmol), Pd₂(dba)₃ (4.7 mg, 5.2 μmol), and Xantphos (4.2 mg, 7.2 μmol). The reaction mixture was then stirred at 90 °C under N₂ for 12 h and concentrated to give a residue. The residue was purified by preparative TLC using 33% EtOH/EtOAc as eluent followed by preparative HPLC to afford **36** (2.2 mg, 2%) as a yellow solid. ¹H NMR (400 MHz, DMSO-*d*₆) δ 9.96 (s, 1H), 8.19 (d, *J* = 7.5 Hz, 1H), 8.16 (s, 1H), 7.92 (s, 1H), 6.68 (dd, *J* = 2.0, 7.6 Hz, 1H), 5.27 (s, 2H), 3.44 (s, 3H), 2.35 (s, 3H), 2.25 (s,

3H). MS-ESI (m/z) calcd for $C_{15}H_{17}N_8O$ [$M + H$] $^+$: 325.1. Found 325.1.

4,5-Dimethyl-N-(2-oxoindolin-5-yl)-4,7-dihydro-tetrazolo[1,5-*a*]-pyrimidine-6-carboxamide (37). To a solution of 5-aminoindolin-2-one (73 mg, 492 μ mol) in 2 mL of DCM were added carboxylic acid **49** (80 mg, 410 μ mol), T3P (50 wt % in EtOAc, 783 mg, 1.23 mmol), and Et_3N (166 mg, 1.64 mmol, 228 μ L). The reaction mixture was then stirred at 25 °C for 12 h. The mixture was concentrated, washed with MeOH (3 mL), filtered, and dried under vacuum to afford **37** (54 mg, 37%) as a white solid. 1H NMR (400 MHz, DMSO- d_6) δ 10.32 (s, 1H) 9.83 (s, 1H) 7.53 (s, 1H) 7.37 (br d, $J = 8.38$ Hz, 1H) 6.75 (d, $J = 8.38$ Hz, 1H) 5.22 (s, 2H) 3.47 (s, 2H) 3.40 (s, 3H) 2.20 (s, 3H). MS-ESI (m/z) calcd for $C_{15}H_{16}N_7O_2$ [$M + H$] $^+$: 326.1. Found 326.2.

4,5-Dimethyl-N-(2-oxo-2,3-dihydro-1H-benzo[d]imidazol-5-yl)-4,7-dihydro-tetrazolo[1,5-*a*]pyrimidine-6-carboxamide (38). To a solution of 5-amino-1,3-dihydro-2H-benzo[d]imidazol-2-one (76 mg, 512 μ mol) in 1 mL of DCM were added carboxylic acid **49** (100 mg, 512 μ mol) and T3P (50 wt % in EtOAc, 489 mg, 768 μ mol). The reaction mixture was then stirred at 20 °C for 30 min. Et_3N (153 mg, 1.54 mmol, 214 μ L) was added, and the reaction mixture was stirred at 20 °C for 12 h. The reaction mixture was washed with CH_3CN (1 mL), saturated aqueous $NaHCO_3$ (1 mL), and H_2O (5 mL) and then concentrated to afford **38** (28 mg, 16%) as a white solid. 1H NMR (400 MHz, DMSO- d_6) δ 10.52 (br s, 3H), 7.46 (s, 1H), 7.08 (br d, $J = 7.5$ Hz, 1H), 6.84 (br d, $J = 7.9$ Hz, 1H), 5.24 (br s, 2H), 3.41 (s, 3H), 2.21 (s, 3H). MS-ESI (m/z) calcd for $C_{14}H_{15}N_8O_2$ [$M + H$] $^+$: 327.1. Found 327.2.

(R)-4,5,7-Trimethyl-N-(1-methyl-2-oxo-2,3-dihydro-1H-benzo[d]imidazol-5-yl)-4,7-dihydro-tetrazolo[1,5-*a*]pyrimidine-6-carboxamide (39). Carboxylic acid **(R)-32** (50 mg, 0.24 mmol) and 5-amino-1-methyl-1,3-dihydro-2H-benzimidazol-2-one (78 mg, 0.48 mmol) were dissolved in 2.5 mL of anhydrous DMF. The solution was then cooled to 0 °C with an ice–water bath, and Et_3N (0.07 mL, 0.48 mmol) and HATU (109 mg, 0.29 mmol) were sequentially added. The mixture was stirred at 0 °C for 5 min and then at r.t. for 18 h. The mixture was diluted with water (20 mL) and extracted with EtOAc. The combined organic layers were dried over Na_2SO_4 , filtered, and concentrated. The material was purified by reversed-phase column chromatography using a 5–60% CH_3CN/H_2O (0.1% formic acid) gradient eluent to afford **39** (32 mg, 37%) as a beige solid. 1H NMR (400 MHz, DMSO- d_6) δ 10.82 (s, 1H), 10.07 (s, 1H), 7.53 (d, $J = 1.32$ Hz, 1H), 7.17 (dd, $J = 8.36, 1.76$ Hz, 1H), 7.03 (d, $J = 8.36$ Hz, 1H), 5.71 (q, $J = 5.87$ Hz, 1H), 3.42 (s, 3H), 3.26 (s, 3H), 2.17 (s, 3H), 1.54 (d, $J = 6.38$ Hz, 3H). MS-ESI (m/z) calcd for $C_{16}H_{19}N_8O_2$ [$M + H$] $^+$: 355.2. Found 355.2.

(R)-4,5,7-Trimethyl-N-(3-methyl-2-oxo-2,3-dihydro-1H-benzo[d]imidazol-5-yl)-4,7-dihydro-tetrazolo[1,5-*a*]pyrimidine-6-carboxamide (40). 5-Amino-3-methyl-1H-benzimidazol-2-one hydrochloride (200 mg, 1 mmol) was passed through a strong cation-exchange column eluting with MeOH followed by 1 M NH_3 in MeOH to afford the free base. The free base (78 mg, 0.48 mmol) and carboxylic acid **(R)-32** (50 mg, 0.24 mmol) were dissolved in 2.5 mL of anhydrous DMF. The solution was then cooled to 0 °C with an ice–water bath, and Et_3N (70 μ L, 0.48 mmol) and HATU (109 mg, 0.29 mmol) were added. The mixture was stirred at 0 °C for 5 min and then at r.t. for 18 h. The reaction mixture was diluted with water (20 mL) and extracted with EtOAc. The combined organic layers were dried over Na_2SO_4 , filtered, and concentrated. The material was purified by reversed-phase column chromatography using a 5–50% CH_3CN/H_2O gradient eluent to afford **40** (37 mg, 43%) as a beige solid. 1H NMR (400 MHz, DMSO- d_6) δ 10.78 (s, 1H), 10.09 (s, 1H), 7.54 (d, $J = 1.32$ Hz, 1H), 7.13 (dd, $J = 8.36, 1.76$ Hz, 1H), 6.93 (d, $J = 8.36$ Hz, 1H), 5.72 (q, $J = 6.16$ Hz, 1H), 3.43 (s, 3H), 3.26 (s, 3H), 2.18 (d, $J = 0.88$ Hz, 3H), 1.55 (d, $J = 6.38$ Hz, 3H). MS-ESI (m/z) calcd for $C_{16}H_{19}N_8O_2$ [$M + H$] $^+$: 355.2. Found 355.2.

(R)-N-(1,3-Dioxoisindolin-5-yl)-4,5,7-trimethyl-4,7-dihydro-tetrazolo[1,5-*a*]pyrimidine-6-carboxamide (41). To a stirred solution of carboxylic acid **(R)-32** (120 mg, 0.573 mmol), 5-aminoisindoline-1,3-dione (111 mg, 0.688 mmol), and TEA (0.32

mL, 2.3 mmol) in DMF (3.3 mL) at 0 °C was added T3P (50% solution in DMF, 0.417 mL, 0.688 mmol). The reaction mixture was stirred at r.t. for 18 h. The mixture was diluted with H_2O (20 mL) and extracted with EtOAc (2×20 mL). The organic phases were combined, dried over Na_2SO_4 , filtered, and then concentrated. The material was purified by preparative HPLC to afford racemic *N*-(1,3-dioxoisindolin-5-yl)-4,5,7-trimethyl-4,7-dihydro-tetrazolo[1,5-*a*]pyrimidine-6-carboxamide (29 mg, 0.082 mmol). 24.4 mg of this racemic mixture was separated by chiral preparative HPLC to afford **41** (second eluting enantiomer, 7.2 mg) as a white solid. 1H NMR (400 MHz, DMSO- d_6) δ 11.24 (br s, 1H), 10.71 (br s, 1H), 8.19 (d, $J = 1.51$ Hz, 1H), 7.93 (dd, $J = 8.28, 1.76$ Hz, 1H), 7.81 (d, $J = 8.28$ Hz, 1H), 5.78 (d, $J = 6.27$ Hz, 1H), 3.45 (s, 3H), 2.20 (d, $J = 0.75$ Hz, 3H), 1.55 (d, $J = 6.27$ Hz, 3H). MS-ESI (m/z) calcd for $C_{16}H_{16}N_7O_3$ [$M + H$] $^+$: 354.1. Found 354.2.

(R)-4,5,7-Trimethyl-N-(1-oxoisindolin-5-yl)-4,7-dihydro-tetrazolo[1,5-*a*]pyrimidine-6-carboxamide (42). To a stirred solution of carboxylic acid **(R)-32** (120 mg, 0.573 mmol), 5-aminoisindolin-1-one (102 mg, 0.688 mmol), and Et_3N (0.32 mL, 2.3 mmol) in DMF (3.3 mL) at 0 °C was added T3P (50% solution in DMF, 0.417 mL, 0.688 mmol). The reaction mixture was stirred at r.t. for 18 h. The mixture was diluted with H_2O (20 mL) and extracted with EtOAc (20 mL). The organic phase was dried over Na_2SO_4 , filtered, and then concentrated. The material was purified by preparative HPLC. The product-containing fractions were collected and lyophilized to give racemic 4,5,7-trimethyl-*N*-(1-oxoisindolin-5-yl)-4,7-dihydro-tetrazolo[1,5-*a*]pyrimidine-6-carboxamide (13 mg, 0.038 mmol) as a white solid. 7.34 mg of this racemic mixture was separated by chiral preparative HPLC to give **42** (second eluting enantiomer, 1.7 mg, 0.01 mmol) as a white solid. 1H NMR (400 MHz, DMSO- d_6) δ 10.46 (s, 1H), 8.41 (s, 1H), 8.00 (s, 1H), 7.58–7.68 (m, 2H), 5.75 (q, $J = 5.80$ Hz, 1H), 4.36 (s, 2H), 3.44 (s, 3H), 2.18 (d, $J = 1.00$ Hz, 3H), 1.55 (d, $J = 6.27$ Hz, 3H). MS-ESI (m/z) calcd for $C_{16}H_{18}N_7O_2$ [$M + H$] $^+$: 340.1. Found 340.2.

(R)-N-(1-Aminoisoquinolin-6-yl)-4,5,7-trimethyl-4,7-dihydro-tetrazolo[1,5-*a*]pyrimidine-6-carboxamide (43). Bis-carbamate **81** (40 mg, 0.073 mmol) was dissolved in 3 mL of DCM. TFA (1 mL) was then added to the solution, and the reaction mixture was stirred for 1.5 h at r.t. Volatiles were removed under reduced pressure, and the crude material was purified by reversed-phase column chromatography using a 5–50% CH_3CN/H_2O (0.1% formic acid) gradient eluent. The white solid obtained was passed through a strong cation-exchange column eluting with 1 M NH_3 in MeOH to afford **43** (13 mg, 51%) as a white solid. 1H NMR (400 MHz, DMSO- d_6) δ 10.39 (s, 1H), 8.07–8.18 (m, 2H), 7.75 (d, $J = 5.94$ Hz, 1H), 7.55 (dd, $J = 9.02, 1.98$ Hz, 1H), 6.83 (d, $J = 5.72$ Hz, 1H), 6.67 (s, 2H), 5.78 (q, $J = 6.16$ Hz, 1H), 3.45 (s, 3H), 2.20 (d, $J = 0.88$ Hz, 3H), 1.56 (d, $J = 6.38$ Hz, 3H). MS-ESI (m/z) calcd for $C_{17}H_{19}N_8O$ [$M + H$] $^+$: 351.2. Found 351.2.

5-Nitro-3-(pyridin-4-yl)-1H-indazole (45). A mixture of indazole **44** (450 mg, 1.86 mmol), 4-pyridylboronic acid (274 mg, 2.23 mmol), KOAc (547 mg, 5.58 mmol), and Pd(Amphos)Cl $_2$ (132 mg, 186 μ mol, 132 μ L) in 6 mL of EtOH and 1.5 mL of H_2O was degassed and purged with N_2 (3 \times). The mixture was then stirred at 100 °C for 16 h under N_2 . The residue was diluted with 2 M HCl (40 mL) and EtOAc (20 mL). A yellow solid formed, which was collected and dried under vacuum to afford **45** (350 mg), which was used without further purification. MS-ESI (m/z) calcd for $C_{12}H_9N_4O_2$ [$M + H$] $^+$: 241.1. Found 240.8.

3-(Pyridin-4-yl)-1H-indazol-5-amine (46). To a solution of **45** (350 mg, 1.46 mmol) in 4 mL of EtOH and 1 mL of H_2O were added Zn (476 mg, 7.29 mmol) and NH_4Cl (390 mg, 7.29 mmol), and the mixture was stirred at 80 °C for 12 h. The mixture was then filtered, and the solid that was collected was dissolved in 10 mL of DMF and filtered. The filtrate was concentrated to yield **46** (220 mg, 56% two steps) as a yellow gum, which was used without further purification. 1H NMR (400 MHz, DMSO- d_6) δ 13.19 (br s, 1H), 8.62 (br d, $J = 6$ Hz, 2H), 7.90 (br d, $J = 6$ Hz, 2H), 7.34 (d, $J = 9$ Hz, 1H), 7.18 (s, 1H), 6.86 (br d, $J = 9$ Hz, 1H), 5.02 (s, 2H). MS-ESI (m/z) calcd for $C_{12}H_{11}N_4$ [$M + H$] $^+$: 211.1. Found 211.1.

Ethyl 4,5-Dimethyl-4H,7H-[1,2,3,4]tetrazolo[1,5-a]pyrimidine-6-carboxylate (48). To a mixture of 5-aminotetrazole monohydrate (36, 606 mg, 5.88 mmol), formaldehyde aqueous solution (36.5–38% in H₂O; 477 mg, 5.88 mmol), and EtOAc (742 μ L, 5.88 mmol) in EtOH (1.5 mL) was added a catalytic amount of acetic acid (84 μ L, 1.5 mmol). The mixture was then heated under microwave irradiation at 120 °C for 10 min. Volatiles were removed under reduced pressure, and the residue was purified on Biotage (C18, 30 g cartridge, reverse phase, H₂O/CH₃CN as eluent, 95:5–60:40) to afford **48** as a white solid (765 mg, 62%). ¹H NMR (400 MHz, DMSO-*d*₆) δ 10.89 (s, 1H) 5.10 (d, *J* = 0.66 Hz, 2H) 4.14 (q, *J* = 7.04 Hz, 2H) 2.35 (s, 3H) 1.25 (t, *J* = 7.04 Hz, 3H). MS-ESI (*m/z*) calcd for C₈H₁₂N₅O₂ [M + H]⁺: 210.1. Found 210.2.

4,5-Dimethyl-4H,7H-[1,2,3,4]tetrazolo[1,5-a]pyrimidine-6-carboxylic Acid (49). To a solution of ester **48** (200 mg, 0.96 mmol) in DMF (4 mL) were added MeI (119 μ L, 1.91 mmol) and Cs₂CO₃ (405 mg, 1.24 mmol), and the mixture was stirred at 50 °C for 1 h. Cooled H₂O (15 mL) was then added, and the mixture was extracted with EtOAc (15 mL). The organic layer was separated, dried over Na₂SO₄, filtered, and concentrated to afford a residue. The residue was purified by silica gel chromatography using a 0–20% EtOAc/cyclohexane gradient eluent to give ethyl 4,5-dimethyl-4,7-dihydro-tetrazolo[1,5-a]pyrimidine-6-carboxylate (95 mg) as a colorless oil. MS-ESI (*m/z*) calcd for C₉H₁₃N₅O₂ [M + H]⁺: 224.1. Found 224.2.

LiOH (54 mg, 1.28 mmol) was added to a solution of ester **48** (95 mg, 0.43 mmol) in an EtOH/THF/H₂O mixture (4:1:0.6, 4.15 mL). The mixture was stirred at 55 °C for 1 h. Subsequently, the mixture was acidified with 1 M HCl and extracted with DCM (10 mL \times 3). The pH of the aqueous layer was brought to pH = 7 with 1 M NaOH and extracted with DCM (10 mL). The combined organic layers were concentrated in vacuo to afford **49** (110 mg, 59%, two steps) as a white solid, which was used without further purification. ¹H NMR (400 MHz, DMSO-*d*₆) δ 12.55 (br s, 1H), 5.06 (s, 2H), 3.42 (s, 3H), 2.52 (s, 3H). MS-ESI (*m/z*) calcd for C₉H₁₃N₅O₂ [M + H]⁺: 196.1. Found 196.1.

N-(3-Bromo-1H-indazol-5-yl)-4,5-dimethyl-4,7-dihydro-tetrazolo[1,5-a]pyrimidine-6-carboxamide (51). To a solution of 3-bromo-1H-indazol-5-amine (**50**) (30 mg, 141 μ mol) and carboxylic acid **49** (27.6 mg, 141 μ mol) in 2 mL of EtOAc were added T3P (50 wt % in EtOAc, 270 mg, 424 μ mol) and Et₃N (78.8 μ L, 566 μ mol). The mixture was then stirred at 60 °C for 12 h and concentrated. The residue was purified by preparative HPLC (with 0.1% TFA) to afford **51** (8.7 mg, 16%) as a yellow solid TFA salt. ¹H NMR (400 MHz, DMSO-*d*₆) δ 13.18–13.54 (m, 1H), 10.09 (s, 1H), 8.08 (s, 1H), 7.51–7.59 (m, 2H), 5.29 (s, 2H), 3.43 (s, 3H), 2.26 (s, 3H). MS-ESI (*m/z*) calcd for C₁₄H₁₄BrN₈O [M + H]⁺: 389.0, 391.0. Found 389.0, 390.9.

Ethyl 4-Allyl-5-methyl-4,7-dihydro-tetrazolo[1,5-a]pyrimidine-6-carboxylate (52). To a solution of ester **48** (2.0 g, 9.6 mmol) in THF (15 mL) was added NaH (574 mg, 14.3 mmol, 60% purity) at 0 °C, and the mixture was stirred at 15 °C for 0.5 h. Allyl bromide (1.50 g, 12.4 mmol, 2.20 mL) was then added at 0 °C. The reaction mixture was stirred at 15 °C for 16 h, quenched with H₂O (100 mL) at 0 °C, and extracted with EtOAc (25 mL \times 3). The combined organic layers were washed with brine (30 mL), dried over Na₂SO₄, filtered, and concentrated to give a residue. The residue was purified by silica gel chromatography using a 0–20% EtOAc/petroleum ether gradient eluent to give **52** (820 mg, 27%) as a yellow oil. MS-ESI (*m/z*) calcd for C₁₁H₁₆N₅O₂ [M + H]⁺: 250.1. Found: 250.3.

4-Allyl-5-methyl-4,7-dihydro-tetrazolo[1,5-a]pyrimidine-6-carboxylic Acid (53). To a solution of compound **52** (820 mg, 2.57 mmol) in EtOH (10 mL) and H₂O (10 mL) was added LiOH·H₂O (324 mg, 7.71 mmol). The mixture was stirred at 15 °C for 16 h and concentrated. The reaction mixture was then acidified with 1 N HCl to pH = 3. The resulting precipitate was collected by filtration to give the product (510 mg, 66%) as a white solid, which was used without further purification. MS-ESI (*m/z*) calcd for C₉H₁₂N₅O₂ [M + H]⁺: 222.1. Found: 222.3.

4-Allyl-N-(1H-indazol-5-yl)-5-methyl-4,7-dihydro-tetrazolo[1,5-a]pyrimidine-6-carboxamide (54). To a stirred solution of carboxylic acid **53** (300 mg, 1.36 mmol) in DCM (3 mL) were added 1H-indazol-5-amine (181 mg, 1.36 mmol) and T3P (50 wt % in EtOAc, 1.29 g, 2.03 mmol), and the reaction mixture was stirred at 20 °C for 0.5 h. Et₃N (412 mg, 4.07 mmol) was then added, and the reaction mixture was stirred at 20 °C for 12 h. The reaction mixture was concentrated, and the residue was purified by preparative HPLC (0.04% NH₄OH/10 mM NH₄HCO₃) to give **54** (230 mg, 50%) as a purple solid. ¹H NMR (400 MHz, DMSO-*d*₆) δ 13.04 (br s, 1H), 10.07 (s, 1H), 8.14 (s, 1H), 8.02 (s, 1H), 7.44–7.51 (m, 2H), 5.88–5.99 (m, 1H), 5.14–5.25 (m, 2H), 4.51 (br d, *J* = 4 Hz, 2H), 3.15 (d, *J* = 5 Hz, 2H), 2.19 (s, 3H). MS-ESI (*m/z*) calcd for C₁₆H₁₇N₈O [M + H]⁺: 337.1. Found: 337.1.

N-(1H-Indazol-5-yl)-5-methyl-4,7-dihydro-tetrazolo[1,5-a]pyrimidine-6-carboxamide (55). Carboxamide **54** (200 mg, 594.62 μ mol), 1,3-dimethylbarbituric acid (186 mg, 1.19 mmol), and Pd(PPh₃)₄ (68.7 mg, 59.5 μ mol) in 10 mL of DCM and 5 mL of EtOH were degassed and then heated to 55 °C for 12 h under N₂. After cooling to 20 °C, the reaction mixture was filtered and the filtrate was concentrated. The residue was purified by prep-HPLC (0.04% NH₄OH/10 mM NH₄HCO₃) to give **55** (100 mg, 57%) as a white solid. MS-ESI (*m/z*) calcd for C₁₃H₁₃N₈O [M + H]⁺: 297.1. Found: 297.3.

3-Bromo-5-nitro-1-((2-(trimethylsilyl)ethoxy)methyl)-1H-indazole (57). To a solution of 3-bromo-5-nitro-1H-indazole (**44**) (400 mg, 1.65 mmol) in DMF (7 mL) at 0 °C was added NaH (60% w/w, 79 mg, 1.98 mmol), and the mixture was stirred for 15 min. SEM-Cl (0.35 mL, 1.98 mmol) was then added, and the reaction mixture was warmed to r.t. and stirred for 2 h. The reaction was carefully quenched with a sat. aq. NH₄Cl, and the mixture was extracted with EtOAc. The combined organic extracts were concentrated to dryness under reduced pressure and purified by silica gel chromatography using a 0–40% EtOAc/cyclohexane gradient eluent to afford **57** (372 mg, 60%) as a white solid. ¹H NMR (400 MHz, CDCl₃) δ 8.66 (d, *J* = 1.8 Hz, 1H), 8.38 (s, 1H), 8.38 (dd, *J* = 2.0, 9.2 Hz, 1H), 7.68 (d, *J* = 9.2 Hz, 1H), 5.76 (s, 2H), 3.68–3.52 (m, 2H), 0.95–0.87 (m, 2H), –0.03 (s, 9H). MS-ESI (*m/z*) calcd for C₁₃H₁₉BrN₃O₃Si [M + H]⁺: 372.0, 374.0. Found 372.2, 374.1.

5-Nitro-3-(4,4,5,5-tetramethyl-1,3,2-dioxaborolan-2-yl)-1-((2-(trimethylsilyl)ethoxy)methyl)-1H-indazole (58). Indazole **57** (372 mg, 1.0 mmol), bis(pinacolato)diboron (279 mg, 1.1 mmol), and KOAc (294 mg, 3.0 mmol) were suspended in 3 mL of 1,4-dioxane. The mixture was purged with N₂ for 5 min, and then Pd(dppf)Cl₂ (36 mg, 0.05 mmol) was added. The resulting mixture was heated to 100 °C for 1 h under a N₂ atmosphere. The mixture was partitioned between water and EtOAc and extracted. The combined organic layers were washed with water, dried over anhydrous Na₂SO₄, and the solvent was removed under reduced pressure to afford **58**, which was used without further purification.

¹H NMR (400 MHz, CDCl₃) δ 9.05 (d, *J* = 2.20 Hz, 1H) 8.32 (dd, *J* = 9.24, 2.20 Hz, 1H) 7.72 (d, *J* = 9.24 Hz, 1H) 5.89 (s, 2H) 3.54–3.61 (m, 2H) 1.46 (s, 12H) 0.86–0.91 (m, 2H) –0.05 (s, 9H). MS-ESI (*m/z*) calcd for C₁₃H₁₉BrN₃O₃Si [M+H-C₆H₁₀]⁺: 338.1. Found 338.2.

4-(4-(5-Nitro-1-((2-(trimethylsilyl)ethoxy)methyl)-1H-indazol-3-yl)pyridin-2-yl)morpholine (59). Boronic ester **58** (crude, 1.0 mmol), 4-(4-bromopyridin-2-yl)morpholine (292 mg, 1.2 mmol), and Cs₂CO₃ (977 mg, 3.0 mmol) were suspended in 5 mL of THF and 1 mL of water. The mixture was purged with N₂ for 5 min, and then Pd(dppf)Cl₂ (73 mg, 0.10 mmol) was added. The reaction mixture was stirred at 100 °C for 1 h under N₂. The mixture was partitioned between water and EtOAc and extracted. The combined organic layers were washed with water, dried over anhydrous Na₂SO₄, and the solvent was removed under reduced pressure. The material was purified by silica gel chromatography using a 0–30% EtOAc/cyclohexane gradient eluent to afford **59** (200 mg, 44%, two steps) as a yellow oil. ¹H NMR (400 MHz, CDCl₃) δ 8.99 (d, *J* = 2.0 Hz, 1H), 8.44–8.35 (m, 2H), 7.74 (d, *J* = 9.2 Hz, 1H), 7.24 (dd, *J* = 1.3, 5.1 Hz, 1H), 7.21 (s, 1H), 5.85 (s, 2H), 3.94–3.88 (m, 4H), 3.70–3.61

(m, 6H), 0.99–0.88 (m, 2H), –0.03 (s, 9H). MS-ESI (m/z) calcd for $C_{22}H_{30}N_5O_4Si$ [$M + H$]⁺: 456.2. Found 456.4.

3-(2-Morpholinopyridin-4-yl)-1-((2-trimethylsilyl)ethoxy)methyl)-1H-indazol-5-amine (60). A mixture of nitroindazole **59** (200 mg, 0.44 mmol), NH_4Cl (26 mg, 0.48 mmol), and iron powder (98 mg, 1.8 mmol) in 4 mL of EtOH/ H_2O (1:1) was stirred at 80 °C for 30 min. The solids were filtered through a celite pad, washing with EtOH. Volatiles were removed under vacuum, and the residue was redissolved in EtOAc. Water was added, and the two phases were separated. The aqueous layer was extracted with EtOAc, and the combined organic layers were washed with water, dried over Na_2SO_4 , and the solvent was removed under reduced pressure to afford **60** (150 mg, 80%). ¹H NMR (400 MHz, $CDCl_3$) δ 8.33 (d, $J = 5.1$ Hz, 1H), 7.47 (d, $J = 8.8$ Hz, 1H), 7.26–7.18 (m, 3H), 6.96 (dd, $J = 2.0, 8.8$ Hz, 1H), 5.74 (s, 2H), 3.94–3.87 (m, 4H), 3.77 (br s, 2H), 3.66–3.60 (m, 6H), 0.99–0.85 (m, 2H), –0.04 (s, 9H). MS-ESI (m/z) calcd for $C_{22}H_{32}N_5O_2Si$ [$M + H$]⁺: 426.2. Found 426.4.

(R)-4,5,7-Trimethyl-N-(3-(2-morpholinopyridin-4-yl)-1-((2-trimethylsilyl)ethoxy)methyl)-1H-indazol-5-yl)-4,7-dihydro-1,5-a]pyrimidine-6-carboxamide (61). Carboxylic acid (**R**)-**32** (35 mg, 0.17 mmol) and amine **60** (71 mg, 0.17 mmol) were dissolved in 2 mL of anhydrous DMF. Then, the solution was cooled to 0 °C with an ice–water bath and Et_3N (0.05 mL, 0.33 mmol) and HATU (76 mg, 0.20 mmol) were added. The mixture was stirred at 0 °C for 5 min, at room temperature overnight, heated at 50 °C for 2 h, and then at 70 °C for an additional 2 h. The mixture was partitioned between water and EtOAc and extracted. The combined organic layers were washed with water, dried over Na_2SO_4 , filtered, and the solvent was removed under vacuum. The material was purified by silica gel chromatography using a 50–100% EtOAc/cyclohexane gradient eluent to afford material of insufficient purity. The material was then further purified by silica gel chromatography (silica gel 110 NH_2) using a 0–80% EtOAc/cyclohexane gradient eluent to afford **61** (35 mg, 33%). ¹H NMR (400 MHz, $CDCl_3$) δ 8.52 (s, 1H), 8.36 (d, $J = 5.1$ Hz, 1H), 8.28 (s, 1H), 7.69–7.57 (m, 2H), 7.28–7.26 (m, 1H), 5.81 (s, 2H), 5.61 (q, $J = 5.9$ Hz, 1H), 3.93–3.83 (m, 4H), 3.70–3.56 (m, 6H), 3.49 (s, 3H), 2.31 (s, 3H), 1.74 (d, $J = 6.4$ Hz, 3H), 1.02–0.86 (m, 2H), 0.00–0.07 (m, 9H). MS-ESI (m/z) calcd for $C_{30}H_{41}N_{10}O_3Si$ [$M + H$]⁺: 617.3. Found 617.4.

Methyl 5,7,7-Trimethyl-4,7-dihydro-1,5-a]pyrimidine-6-carboxylate (64). A mixture of 5-aminotetrazole monohydrate (**63**) (66 mg, 0.64 mmol) and methyl 2-acetyl-3-methyl-2-butenolate¹⁶ (**62**) (100 mg, 0.64 mmol) was heated in 5 mL of EtOH in the presence of molecular sieves for 4 h at reflux. The reaction was cooled to r.t., filtered, and concentrated to afford **64** (80 mg, 56%) as a white solid, which was used without further purification. ¹H NMR (400 MHz, $DMSO-d_6$) δ 10.70 (s, 1H), 3.79–3.88 (m, 3H), 2.38–2.48 (m, 3H), 1.94–2.02 (m, 6H). MS-ESI (m/z) calcd for $C_9H_{14}N_5O_2$ [$M + H$]⁺: 224.1. Found 224.3.

Methyl 4,5,7,7-Tetramethyl-4,7-dihydro-1,5-a]pyrimidine-6-carboxylate (65). To a solution of methyl ester **64** (73 mg, 0.33 mmol) in DMF (5 mL) were added MeI (0.12 mL, 2.0 mmol) and Cs_2CO_3 (699 mg, 2.0 mmol), and the mixture was stirred at 50 °C for 0.5 h. The solvent was evaporated, and the material was extracted with water and EtOAc. The organic layer was separated, dried over Na_2SO_4 , filtered, and concentrated to afford **65** (75 mg, 97%) as a white solid, which was used without further purification. ¹H NMR (400 MHz, $DMSO-d_6$) δ 4.84 (s, 1H), 3.76–3.88 (m, 3H), 3.47–3.58 (m, 3H), 2.21–2.32 (m, 3H), 1.78–1.92 (m, 6H). MS-ESI (m/z) calcd for $C_{10}H_{16}N_5O_2$ [$M + H$]⁺: 238.1. Found 238.2.

4,5,7,7-Tetramethyl-4,7-dihydro-1,5-a]pyrimidine-6-carboxylic Acid (66). To a solution of methyl ester **65** (75 mg, 0.32 mmol) in 2.0 mL of THF was added a solution of LiOH (39 mg, 0.93 mmol) in H_2O (2 mL). The mixture was stirred at 50 °C for 15 h. The solvent was evaporated, and the remaining aqueous solution was acidified with 1 M HCl to pH = 1, extracted with EtOAc, dried over Na_2SO_4 , filtered, and evaporated to afford **66** (118 mg) as a colorless oil, which was of sufficient purity for further elaboration. ¹H NMR (400 MHz, $DMSO-d_6$) δ 3.34–3.39 (m, 3H), 1.90 (s, 3H), 1.64–1.71

(m, 6H). MS-ESI (m/z) calcd for $C_9H_{14}N_5O_2$ [$M + H$]⁺: 224.1. Found 224.2.

tert-Butyl 5-(4,5,7,7-Tetramethyl-4,7-dihydro-1,5-a]pyrimidine-6-carboxamido)-1H-indazole-1-carboxylate (67). Carboxylic acid **66** (60 mg, 0.27 mmol) was dissolved in 2 mL of DMF, and Et_3N (0.075 mL, 0.54 mmol), N -(1-Boc-5-aminoindazole (53.8 mg, 0.4 mmol), and HATU (103 mg, 0.27 mmol) were added. The reaction mixture was then stirred at r.t. for 1 h. The solvent was evaporated, and the residue was extracted with EtOAc and water. The organic layer was separated, dried over Na_2SO_4 , filtered, and concentrated. The material was purified by preparative HPLC to afford **67** (7.5 mg) as a white solid. ¹H NMR (400 MHz, $DMSO-d_6$) δ 8.44 (br s, 1H), 8.04–8.22 (m, 3H), 7.45–7.57 (m, 1H), 3.52 (s, 3H), 1.90–1.99 (m, 3H), 1.72–1.77 (m, 9H), 1.59 (s, 6H). MS-ESI (m/z) calcd for $C_{21}H_{27}N_8O_3$ [$M + H$]⁺: 439.2. Found 439.8.

2-(Bromomethyl)-5-nitropyridine (69). To a solution of 2-methyl-5-nitropyridine (**68**) (5.0 g, 36 mmol) in CCl_4 (75 mL) were added benzoyl peroxide (1.75 g, 7.24 mmol) and NBS (7.09 g, 39.82 mmol). The mixture was stirred at 80 °C for 12 h and then concentrated. The material was purified by column chromatography using a 0–10% EtOAc/petroleum ether gradient eluent to afford **69** (2.5 g, 31%) as a yellow oil. ¹H NMR (400 MHz, $CDCl_3$) δ 9.38 (d, $J = 3$ Hz, 1H), 8.49 (dd, $J = 9, 3$ Hz, 1H), 7.67 (d, $J = 9$ Hz, 1H), 4.61 (s, 2H). MS-ESI (m/z) calcd for $C_6H_6BrN_2O_2$ [$M + H$]⁺: 217.0, 219.0. Found 217.0, 219.0.

(5-Nitropyridin-2-yl)methanamine (70). To a mixture of $NH_3 \cdot H_2O$ (10 mL) and dioxane (30 mL) was added nitropyridine **69** (2.45 g, 11.3 mmol) in dioxane (10 mL). The resulting mixture was stirred at 25 °C for 2 h. The reaction mixture was then concentrated to afford **70** (1.70 g) as a brown oil, which was used without further purification. MS-ESI (m/z) calcd for $C_6H_8N_3O_2$ [$M + H$]⁺: 154.1. Found 154.1.

3-Methyl-6-nitroimidazo[1,5-a]pyridine (71). To a solution of methanamine **70** (1.70 g, 11 mmol) in Ac_2O (30 mL) was added PTSA (1.91 g, 11.1 mmol). The mixture was stirred at 100 °C for 2 h. The reaction mixture was cooled to 25 °C, poured into ice water (100 mL), and extracted with EtOAc (50 mL \times 3). The combined organic layers were dried over Na_2SO_4 , filtered, and concentrated. The material was purified by column chromatography using a 0–50% EtOAc/petroleum ether gradient eluent to afford **71** (650 mg, 32%, two steps) as a red solid. ¹H NMR (400 MHz, $CDCl_3$) δ 8.81 (s, 1H), 7.36–7.45 (m, 2H), 7.27–7.35 (m, 1H), 2.70 (s, 3H). MS-ESI (m/z) calcd for $C_8H_8N_3O_2$ [$M + H$]⁺: 178.1. Found 178.1.

3-Methylimidazo[1,5-a]pyridin-6-amine (72). To a solution of nitroimidazopyridine **71** (70 mg, 395 μ mol) in 60 mL of MeOH was added 10% Pd/C (110 mg). The mixture was degassed and purged with H_2 (3 \times) and stirred at 25 °C for 0.5 h under a H_2 atmosphere (15 psi). The reaction mixture was filtered, and the filtrate was concentrated to afford **72** (50 mg) as a green oil, which was used without further purification. MS-ESI (m/z) calcd for $C_8H_{10}N_3$ [$M + H$]⁺: 148.1. Found 148.3.

1-(4-Bromopyridin-2-yl)ethan-1-amine (74). Into a 100 mL three-necked, round-bottom flask, purged and maintained with an inert atmosphere of nitrogen, was placed a solution of MeMgBr (3 M, 16.39 mL) in 25 mL of THF. A solution of 4-bromopyridine-2-carbonitrile (**73**) (3 g, 16.39 mmol) in 15 mL of THF was added dropwise at 25 °C over 30 min. MeOH (10 mL) was then added dropwise followed by addition of $NaBH_4$ (3.10 g, 81.96 mmol) in five portions. The resulting mixture was stirred at 25 °C for 2 h and diluted with EtOAc (40 mL) and H_2O (30 mL) at 0 °C. The pH was brought to 9 with 1 M NaOH, and the solid was removed by filtration. The filtrate was extracted with EtOAc, and the combined organic layers were concentrated to afford **74** (3.1 g, 94%) as a yellow oil, which was used without further purification. MS-ESI (m/z) calcd for $C_7H_{10}BrN_2$ [$M + H$]⁺: 201.0, 203.0. Found 201.0, 203.0.

N -(1-(4-Bromopyridin-2-yl)ethyl)formamide (75). To a solution of 1-(4-bromopyridin-2-yl)ethan-1-amine (**74**) (3.1 g, 15 mmol) and ethyl formate (1.14 g, 15.4 mmol) in 30 mL of toluene was added $AlMe_3$ (2.0 M in toluene, 7.7 mL). The mixture was stirred at 90 °C for 5 h and quenched by the addition of 15 mL of H_2O at 0 °C. The

mixture was then concentrated, and the residue was diluted with MeOH (50 mL) and filtered. The filtrate was concentrated and purified by silica gel chromatography using a 0–100% EtOAc/petroleum ether gradient eluent to afford **75** (410 mg, 10%) as a brown oil. ^1H NMR (400 MHz, CDCl_3) δ 8.34 (d, $J = 5.2$ Hz, 1H), 8.21 (s, 1H), 7.45–7.38 (m, 2H), 7.02–7.00 (m, 1H), 5.21–5.14 (m, 1H), 1.49 (d, $J = 6.8$ Hz, 3H). MS-ESI (m/z) calcd for $\text{C}_8\text{H}_{10}\text{BrN}_2\text{O}$ [$\text{M} + \text{H}$] $^+$: 229.0, 231.0. Found 228.9, 230.8.

7-Bromo-1-methylimidazo[1,5-*a*]pyridine (76). To a solution of *N*-(1-(4-bromopyridin-2-yl)ethyl)formamide (**75**) (410 mg, 1.8 mmol) in 4 mL of toluene was added POCl_3 (549 mg, 3.58 mmol, 333 μL) under N_2 , and the mixture was stirred at 80 $^\circ\text{C}$ for 2 h. The pH was brought to 10 carefully with saturated aqueous Na_2CO_3 at 0 $^\circ\text{C}$ and extracted with EtOAc (30 mL \times 3). The combined organic layers were concentrated in vacuo to afford **76** (350 mg, 93%) as a brown solid, which was used without further purification. MS-ESI (m/z) calcd for $\text{C}_8\text{H}_8\text{BrN}_2$ [$\text{M} + \text{H}$] $^+$: 211.0, 213.0. Found 210.9, 213.0.

4,5-Dimethyl-4,7-dihydro-tetrazolo[1,5-*a*]pyrimidine-6-carboxamide (77). To a solution of carboxylic acid **49** (2.0 g, 10 mmol) in 40 mL of THF was added CDI (1.83 g, 11.3 mmol). The mixture was stirred at 20 $^\circ\text{C}$ for 1.5 h and then $\text{NH}_3 \cdot \text{H}_2\text{O}$ (7.18 g, 51.2 mmol, 7.89 mL, 25% purity) was added, and the reaction mixture was stirred at 20 $^\circ\text{C}$ for 0.25 h. The reaction mixture was concentrated and purified by preparative HPLC to give **77** (0.1 g, 5%) as a white solid. MS-ESI (m/z) calcd for $\text{C}_7\text{H}_{11}\text{N}_6\text{O}$ [$\text{M} + \text{H}$] $^+$: 195.1. Found 195.0.

tert-Butyl (tert-Butoxycarbonyl)(6-nitroisoquinolin-1-yl)-carbamate (79). A suspension of 6-nitroisoquinolin-1-amine (**78**) (110 mg, 0.54 mmol), di-*tert*-butyl dicarbonate (335 mg, 1.53 mmol), and DMAP (3.5 mg) in 3.0 mL of CH_3CN was stirred at 70 $^\circ\text{C}$ for 1 h. Volatiles were then removed under reduced pressure, and the residue was purified by silica gel chromatography using a 0–20% EtOAc/cyclohexane gradient eluent. Product-containing fractions were combined to afford **79** (160 mg, 70%) as a pale yellow solid. ^1H NMR (400 MHz, CDCl_3) δ 8.84 (d, $J = 2.0$ Hz, 1H), 8.64 (d, $J = 5.5$ Hz, 1H), 8.41 (dd, $J = 2.2, 9.0$ Hz, 1H), 8.17 (d, $J = 9.2$ Hz, 1H), 7.88 (d, $J = 5.7$ Hz, 1H), 1.36 (s, 18H). MS-ESI (m/z) calcd for $\text{C}_{19}\text{H}_{24}\text{N}_3\text{O}_6$ [$\text{M} + \text{H}$] $^+$: 390.2. Found 390.2.

tert-Butyl (6-Aminoisoquinolin-1-yl)(tert-butoxycarbonyl)-carbamate (80). Carbamate **79** (160 mg, 0.41 mmol) was dissolved in 5.0 mL of EtOH, and 10% Pd/C (50 mg) was added. The mixture was left to react under H_2 (1 atm) at room temperature for 90 min. The catalyst was then removed by filtration, washing with EtOH. The filtrate was concentrated and dried under reduced pressure to afford **80** (143 mg, 97%) as an off-white solid. ^1H NMR (400 MHz, $\text{DMSO}-d_6$) δ 8.04 (d, $J = 5.7$ Hz, 1H), 7.50 (d, $J = 9.0$ Hz, 1H), 7.38 (d, $J = 5.7$ Hz, 1H), 7.05 (dd, $J = 2.1, 8.9$ Hz, 1H), 6.78 (d, $J = 2.0$ Hz, 1H), 6.06 (s, 2H), 1.31 (s, 18H). MS-ESI (m/z) calcd for $\text{C}_{19}\text{H}_{26}\text{N}_4\text{O}_4$ [$\text{M} + \text{H}$] $^+$: 360.2. Found 360.4.

tert-Butyl (R)-(tert-Butoxycarbonyl)(6-(4,5,7-trimethyl-4,7-dihydro-tetrazolo[1,5-*a*]pyrimidine-6-carboxamido)isoquinolin-1-yl)carbamate (81). Carboxylic acid (**R**)-**32** (55 mg, 0.26 mmol) and *bis*-carbamate **80** (114 mg, 0.32 mmol) were dissolved in 0.5 mL of pyridine (0.5 mL). EDCI (61 mg, 0.32 mmol) and DMAP (3 mg, 0.025 mmol) were then added. The resulting solution was stirred at 70 $^\circ\text{C}$ for 16 h. The mixture was diluted with EtOAc and washed with water (3 \times) and brine (1 \times). The organic layer was dried over anhydrous Na_2SO_4 and evaporated to dryness under reduced pressure. The crude material was purified by reversed-phase column chromatography using a 0–60% $\text{CH}_3\text{CN}/\text{H}_2\text{O}$ gradient eluent (0.1% formic acid) followed by silica gel chromatography (silica gel 110 NH_2) using a 50–100% EtOAc/cyclohexane gradient eluent to afford **81** (43 mg, 29%) as a white solid. ^1H NMR (400 MHz, $\text{DMSO}-d_6$) δ 10.63 (s, 1H), 8.49 (d, $J = 1.8$ Hz, 1H), 8.33 (d, $J = 5.7$ Hz, 1H), 7.91–7.77 (m, 3H), 5.81 (q, $J = 6.2$ Hz, 1H), 3.45 (s, 3H), 2.22 (s, 3H), 1.57 (d, $J = 6.4$ Hz, 3H), 1.31 (s, 18H). MS-ESI (m/z) calcd for $\text{C}_{27}\text{H}_{35}\text{N}_8\text{O}_5$ [$\text{M} + \text{H}$] $^+$: 551.3. Found 551.3.

LRRK2 Biochemical Assays. Biochemical tests were carried out using purified truncated LRRK2 enzymes (WT and G2019S) and reagents from LifeTechnologies. Inhibition of LRRKtide substrate phosphorylation was assessed using a homogeneous time-resolved

fluorescence (HTRF) assay. Briefly, a 2 nM nominal concentration of enzymes was preincubated for 15 min with inhibitors before the addition of 0.4 μM LRRKtide and 25 μM ATP. Assays were carried out in a 384-well plate in a final volume of 10 μL . After 1 h incubation, the reaction was stopped with a LanthaScreen time-resolved (TR-FRET) Dilution Buffer containing 10 mM ethylenediamine tetraacetic acid (EDTA) and 2 nM Tb-anti-pERM-(pLRRKtide) Ab, and HTRF signal was read in an Envision reader.

pS935-LRRK2 Cellular Assays. HEK293 cells stably transfected with human LRRK2 or the G2019S variant of human LRRK2 (HEK/WT-LRRK2 and HEK/G2019S-LRRK2 lines) were seeded into 384-well poly-D-lysine-coated plates at a density of 5K cell/well in 50 μL of DMEM medium supplemented with 1% serum. LRRK2 inhibitors (0.25 μM) in DMSO were added using an acoustic dispenser. After 2 h incubation at 37 $^\circ\text{C}$, the medium was removed, and phospho-LRRK2 (Ser935) kit reagents from CisBio were added following the manufacturer's instructions. HTRF signal was read using an Envision reader.

pS1292-LRRK2 Cellular Assays. HEK/WT-LRRK2 or HEK/G2019S-LRRK2 cells were seeded into 96-well poly-D-lysine-coated plates at a density of 30–50K cell/well in 100 μL of DMEM medium supplemented with 1% serum. After addition of 1 μL of test article in 100% DMSO, an additional 100 μL of medium was added to each well. After 2 h incubation at 37 $^\circ\text{C}$, the medium was removed, and after washing with phosphate-buffered saline (PBS), Lysis Buffer plus phosphatase inhibitors were added. After shaking for 1 h at 4 $^\circ\text{C}$, lysates were transferred into MSD assay plates precoated with mouse monoclonal anti-LRRK2 antibody at a concentration of 1 $\mu\text{g}/\text{mL}$ for 1 h at r.t. Plates were sealed and incubated overnight at 4 $^\circ\text{C}$, with shaking. The unbound proteins were removed by washing plates with TBST. Rabbit anti-pS1292 antibody diluted 1:400 in 1% Blocker A/TBST was added and incubated for 2 h at r.t. with shaking. The antibody was removed by washing, and MSD Sulfo-Tag labeled antirabbit diluted 1:500 in 3% Blocker A/TBST was added and incubated in the dark for 1 h at RT, with shaking. The antibody solution was removed by washing plates, and Read Buffer was added. Plates were read immediately in a MSD reader (e.g., MSD Sector 6000).

pThr73-Rab10 and pS935-LRRK2 Cellular Immunoblot-Based Assays. HEK/WT-LRRK2 or HEK/G2019S-LRRK2 cells were seeded into 24-well plates (Corning 353047) at 100 000 cells/well in 500 μL EMEM media containing 1% FBS. Approximately 24 h after plating, cells were treated with 250 μL EMEM media containing 1% FBS and 3.75 μL test article in 100% DMSO. After a 2 h incubation, cells were washed with DPBS, and 50 μL of lysis buffer was added to each well. Lysis buffer contained 1% sodium dodecyl sulfate (SDS), 25 μM Tris pH 7.4, 137 μM NaCl, and 2.7 μM KCl in water supplemented with protease inhibitors (Thermo Scientific, 78425) and phosphatase inhibitors (G Biosciences, 786–452; G Biosciences, 786–782). After incubating the plate on an orbital shaker for 5 min at 800 rpm at RT, the cell lysates were collected, heated at 65 $^\circ\text{C}$ for 10 min, and load dye (Cell signaling, 7722S) was added according to the manufacturer's instructions. Levels of pThr73-Rab10, total Rab10, pS935-LRRK2, and total LRRK2 were quantified from immunoblots. For pS935 and total LRRK2, samples were diluted 1:30 and 8 μL of sample was separated by sodium dodecyl sulfate polyacrylamide gel electrophoresis (SDS-PAGE). For pThr73-Rab10 and total Rab10, 10 μL of sample was separated by SDS-PAGE. Antibodies were used at the following dilutions: LRRK2 total antibody (1:10 000, Antibodies Incorporated, cat #75–253), pS935 antibody (1:2000, Abcam, ab133450), rab10 total antibody (1:2000, United States Biological, 030583), and pRab10 antibody (1:500, Abcam, ab230261).

Pharmacokinetics. Following intravenous bolus and oral gavage administration of compound to fasted male CD-1 mice, blood samples were collected at 0.25, 0.5, 1, 2, 4, 8, and 12 h from the saphenous vein into polypropylene tubes at each time point, blood was transferred to EDTA-K2 tubes, and plasma was prepared by centrifugation. Brain samples were homogenized with 4 volumes (w/v) of 15 mM PBS/ACN (2:1). Levels of EB-42486 in plasma and

brain samples were determined by liquid chromatography and tandem mass spectrometry analyses (LC-MS/MS). Plasma PK profile was analyzed by noncompartmental approaches using Phoenix WinNonlin 6.3 software program.

■ ASSOCIATED CONTENT

SI Supporting Information

The Supporting Information is available free of charge at <https://pubs.acs.org/doi/10.1021/acs.jmedchem.0c01243>.

Compound 1 homology model (PDB)

Molecular formula strings (CSV)

Kinase panel for compound 31 (CSV)

Crystal data for compound (R)-32; ¹H NMR and HPLC traces for compounds 1, 4, 7, 19, 20, 21, 22, 23, 25, 26, 30, and 31; and table of geometric mean and geometric standard deviation of biochemical potency (PDF)

■ AUTHOR INFORMATION

Corresponding Author

Albert W. Garofalo – ESCAPE Bio, South San Francisco, California 94080, United States; orcid.org/0000-0002-1837-417X; Phone: 650-431-0140; Email: garofaloa@escapebio.com

Authors

Jessica Bright – ESCAPE Bio, South San Francisco, California 94080, United States

Stéphane De Lombaert – ESCAPE Bio, South San Francisco, California 94080, United States

Alyssa M. A. Toda – ESCAPE Bio, South San Francisco, California 94080, United States

Kerry Zobel – ESCAPE Bio, South San Francisco, California 94080, United States

Daniele Andreotti – Aptuit, an Evotec Company, Verona 37135, Italy

Claudia Beato – Aptuit, an Evotec Company, Verona 37135, Italy

Silvia Bernardi – Aptuit, an Evotec Company, Verona 37135, Italy

Federica Budassi – Aptuit, an Evotec Company, Verona 37135, Italy

Laura Caberlotto – Aptuit, an Evotec Company, Verona 37135, Italy

Peng Gao – WuXi AppTec, Tianjin 300456, P. R. China

Cristiana Griffante – Aptuit, an Evotec Company, Verona 37135, Italy

Xinying Liu – WuXi AppTec, Tianjin 300456, P. R. China

Luisa Mengatto – Aptuit, an Evotec Company, Verona 37135, Italy

Marco Migliore – Aptuit, an Evotec Company, Verona 37135, Italy

Fabio Maria Sabbatini – Aptuit, an Evotec Company, Verona 37135, Italy

Anna Sava – Aptuit, an Evotec Company, Verona 37135, Italy

Elena Serra – Aptuit, an Evotec Company, Verona 37135, Italy

Paolo Vincetti – Aptuit, an Evotec Company, Verona 37135, Italy

Mingliang Zhang – WuXi AppTec, Tianjin 300456, P. R. China

Holly Carlisle – ESCAPE Bio, South San Francisco, California 94080, United States

Complete contact information is available at:

<https://pubs.acs.org/10.1021/acs.jmedchem.0c01243>

Notes

The authors declare no competing financial interest.

■ ABBREVIATIONS USED

CDI, 1,1'-carbonyldiimidazole; Cl, clearance; DMEM, Dulbecco's modified Eagle's medium; EDCl, 1-ethyl-3-(3-dimethylaminopropyl)carbodiimide; HPK1, hematopoietic progenitor kinase 1; IVB, in vitro biochemical; JNK1, c-Jun N-terminal kinase 1; JNK2, c-Jun N-terminal kinase 2; JNK3, c-Jun N-terminal kinase 3; LRRK2, leucine-rich repeat kinase 2; MPO, multiparameter optimization; MRT, mean residence time; ND, not determined; PD, Parkinson's disease; PTSA, *p*-toluenesulfonic acid; T3P, propylphosphonic anhydride; TTK, dual specificity protein kinase TTK; YSK, serine/threonine-protein kinase 25

■ REFERENCES

- (1) (a) Paisán-Ruiz, C.; Jain, S.; Evans, E. W.; Gilks, W. P.; Simon, J.; van der Brug, M.; Lopez de Munain, A.; Aparicio, S.; Gil, A. M.; Khan, N.; Johnson, J.; Martinez, J. R.; Nicholl, D.; Carrera, I. M.; Pena, A. S.; de Silva, R.; Lees, A.; Marti-Masso, J. F.; Perez-Tur, J.; Wood, N. W.; Singleton, A. B. Cloning of the gene containing mutations that cause PARK8-linked Parkinson's disease. *Neuron* **2004**, *44*, 595–600. (b) Zimprich, A.; Biskup, S.; Leitner, P.; Lichtner, P.; Farrer, M.; Lincoln, S.; Kachergus, J.; Hulihan, M.; Uitti, R. J.; Calne, D. B.; Stoessl, A. J.; Pfeiffer, R. F.; Patenge, N.; Carbajal, I. C.; Vieregge, P.; Asmus, F.; Müller-Myhok, B.; Dickson, D. W.; Meitinger, T.; Strom, T. M.; Wszolek, Z. K.; Gasser, T. Mutations in LRRK2 cause autosomal-dominant parkinsonism with pleomorphic pathology. *Neuron* **2004**, *44*, 601–607. (c) Paisán-Ruiz, C.; Lewis, P. A.; Singleton, A. B. LRRK2: Cause, risk, and mechanism. *J. Parkinson's Dis.* **2013**, *3*, 85–103.
- (2) (a) Monfrini, E.; Di Fonzo, A. Leucine-rich repeat kinase (LRRK2) genetics and Parkinson's Disease. *Adv. Neurobiol.* **2017**, *14*, 3–30. (b) Tolosa, E.; Vila, M.; Klein, C.; Rascol, O. LRRK2 in Parkinson disease: challenges of clinical trials. *Nat. Rev. Neurol.* **2020**, *16*, 97–107.
- (3) Sheng, Z.; Zhang, S.; Bustos, D.; Kleinheinz, T.; Le Pichon, C. E.; Dominguez, S. L.; Solanoy, H. O.; Drummond, J.; Zhang, X.; Ding, X.; Cai, F.; Song, Q.; Li, X.; Yue, Z.; van der Brug, M. P.; Burdick, D. J.; Gunzner-Toste, J.; Chen, H.; Liu, X.; Estrada, A. A.; Sweeney, Z. K.; Searce-Levie, K.; Moffat, J. G.; Kirkpatrick, D. S.; Zhu, H. Ser1292 autophosphorylation is an indicator of LRRK2 kinase activity and contributes to the cellular effects of PD mutations. *Sci. Transl. Med.* **2012**, *4*, No. 164ra161.
- (4) (a) Herzig, M. C.; Kolly, C.; Persohn, E.; Theil, D.; Schweizer, T.; Hafner, T.; Stemmelen, C.; Troxler, T. J.; Schmid, P.; Danner, S.; Schnell, C. R.; Mueller, M.; Kinzel, B.; Grevot, A.; Bolognani, F.; Stirn, M.; Kuhn, R. R.; Kaupmann, K.; van der Putten, P. H.; Rovelli, G.; Shimshek, D. R. LRRK2 protein levels are determined by kinase function and are crucial for kidney and lung homeostasis in mice. *Hum. Mol. Genet.* **2011**, *20*, 4209–4223. (b) Tong, Y.; Yamaguchi, H.; Giaime, E.; Boyle, S.; Kopan, R.; Kelleher, R. J., III; Shen, J. Loss of leucine-rich repeat kinase 2 causes impairment of protein degradation pathways, accumulation of alpha-synuclein, and apoptotic cell death in aged mice. *Proc. Natl. Acad. Sci. U.S.A.* **2010**, *107*, 9879–9884.
- (5) (a) Ness, D.; Ren, Z.; Gardai, S.; Sharpnack, D.; Johnson, V. J.; Brennan, R. J.; Brigham, E. F.; Olaharski, A. J. Leucine-rich repeat kinase 2 (LRRK2)-deficient rats exhibit renal tubule injury and perturbations in metabolic and immunological homeostasis. *PLoS One* **2013**, *8*, No. e66164. (b) Baptista, M. A.; Dave, K. D.; Frasier, M. A.; Sherer, T. B.; Greeley, M.; Beck, M. J.; Varsho, J. S.; Parker, G. A.; Moore, C.; Churchill, M. J.; Meshul, C. K.; Fiske, B. K. Loss of leucine-rich repeat kinase 2 (LRRK2) in rats leads to progressive

abnormal phenotypes in peripheral organs. *PLoS One* **2013**, *8*, No. e80705.

(6) (a) Andersen, M. A.; Wegener, K. M.; Larsen, S.; Badolo, L.; Smith, G. P.; Jeggo, R.; Jensen, P. H.; Sotty, F.; Christensen, K. V.; Thougard, A. PFE-360-induced LRRK2 inhibition induces reversible, non-adverse renal changes in rats. *Toxicology* **2018**, *395*, 15–22. (b) Fell, M. J.; Mirescu, C.; Basu, K.; Cheewatrakoolpong, B.; DeMong, D. E.; Ellis, J. M.; Hyde, L. A.; Lin, Y.; Markgraf, C. G.; Mei, H.; Miller, M.; Poulet, F. M.; Scott, J. D.; Smith, M. D.; Yin, Z.; Zhou, X.; Parker, E. M.; Kennedy, M. E.; Morrow, J. A. MLI-2, a potent, selective, and centrally active compound for exploring the therapeutic potential and safety of LRRK2 kinase inhibition. *J. Pharmacol. Exp. Ther.* **2015**, *355*, 397.

(7) (a) Fuji, R. N.; Flagella, M.; Baca, M.; Baptista, M. A.; Brodbeck, J.; Chan, B. K.; Fiske, B. K.; Honigberg, L.; Jubb, A. M.; Katavolos, P.; Lee, D. W.; Lewin-Koh, S. C.; Lin, T.; Liu, X.; Liu, S.; Lyssikatos, J. P.; O'Mahony, J.; Reichelt, M.; Roose-Girma, M.; Sheng, Z.; Sherer, T.; Smith, A.; Solon, M.; Sweeney, Z. K.; Tarrant, J.; Urkowitz, A.; Warming, S.; Yaylaoglu, M.; Zhang, S.; Zhu, H.; Estrada, A. A.; Watts, R. J. Effect of selective LRRK2 kinase inhibition on nonhuman primate lung. *Sci. Transl. Med.* **2015**, *7*, No. 273ra15. (b) Baptista, M. A. S.; Merchant, K.; Barrett, T.; Bhargava, S.; Bryce, D. K.; Ellis, J. M.; Estrada, A. A.; Fell, M. J.; Fiske, B. K.; Fuji, R. N.; Galatsis, P.; Henry, A. G.; Hill, S.; Hirst, W.; Houle, C.; Kennedy, M. E.; Liu, X.; Maddess, M. L.; Markgraf, C.; Mei, H.; Meier, W. A.; Needle, E.; Ploch, S.; Royer, C.; Rudolph, K.; Sharma, A. K.; Stepan, A.; Steyn, S.; Trost, C.; Yin, Z.; Yu, H.; Wang, X.; Sherer, T. B. LRRK2 inhibitors induce reversible changes in nonhuman primate lungs without measurable pulmonary deficits. *Sci. Transl. Med.* **2020**, *12*, No. eaav0820.

(8) (a) Di Fonzo, A.; Rohé, C. F.; Ferreira, J.; Chien, H. F.; Vacca, L.; Stocchi, F.; Guedes, L.; Fabrizio, E.; Manfredi, M.; Vanacore, N.; Goldwurm, S.; Breedveld, G.; Sampaio, C.; Meco, G.; Barbosa, E.; Oostra, B. A.; Bonifati, V. A frequent LRRK2 gene mutation associated with autosomal dominant Parkinson's disease. *Lancet* **2005**, *365*, 412–415. (b) Kestenbaum, M.; Alcalay, R. N. Clinical Features of LRRK2 Carriers with Parkinson's Disease. In *Leucine-Rich Repeat Kinase 2 (LRRK2)*; Rideout, H. J., Ed.; Advances in Neurobiology 14; Springer: Cham, Switzerland, 2017; p 36.

(9) The Aptuit library is now part of Evotec's screening collection. See Evotec hit identification website: <https://www.evotec.com/en/execute/drug-discovery-services/hit-identification> (accessed May 2020).

(10) Wagner, T. T.; Hou, X.; Verhoest, P. R.; Villalobos, A. Moving beyond rules: the development of a central nervous system multiparameter optimization (CNS MPO) approach to enable alignment of druglike properties. *ACS Chem. Neurosci.* **2010**, *1*, 435–449.

(11) MLI-2 PDB code: SOPB; as of Jan. 2020, there were over 70 indazole-containing kinase inhibitor structures in the PDB with an indazole contributing the key hinge binding interactions.

(12) Dudek, E. P.; Dudek, G. O. Proton magnetic resonance spectra of thiocarboxamides. *J. Org. Chem.* **1967**, *32*, 823.

(13) Sheng, Z.; Zhang, S.; Bustos, D.; Kleinheinz, T.; Le Pichon, C. E.; Dominguez, S. L.; Solanoy, H. O.; Drummond, J.; Zhang, X.; Ding, X.; Cai, F.; Song, Q.; Li, X.; Yue, Z.; van der Brug, M. P.; Burdick, D. J.; Gunzner-Toste, J.; Chen, H.; Liu, X.; Estrada, A. A.; Sweeney, Z. K.; Scearce-Levie, K.; Moffat, J. G.; Kirkpatrick, D. S.; Zhu, H. Ser1292 autophosphorylation is an indicator of LRRK2 kinase activity and contributes to the cellular effects of PD mutations. *Sci. Transl. Med.* **2012**, *4*, No. 164ra161.

(14) Dzamko, N.; Deak, M.; Hentati, F.; Reith, A. D.; Prescott, A. R.; Alessi, D. R.; Nichols, R. J. Inhibition of LRRK2 kinase activity leads to dephosphorylation of Ser⁹¹⁰/Ser⁹³⁵, disruption of 14-3-3 binding and altered cytoplasmic localization. *Biochem. J.* **2010**, *430*, 405.

(15) Raju, C.; Madhaiyan, K.; Uma, R.; Sridhar, R.; Ramakrishna, S. Antimicrobial and antioxidant activity evaluation of tetrazolo[1,5-

a]pyrimidines: A simple diisopropylammonium trifluoroacetate mediated synthesis. *RSC Adv.* **2012**, *2*, 11657–11663.

(16) Nishimura, Y.; Okamoto, Y.; Ikunaka, M.; Ohyama, Y. Synthetic studies on novel 1,4-dihydro-2-methylthio-4,4,6-trisubstituted pyrimidine-5-carboxylic acid esters and their tautomers. *Chem. Pharm. Bull.* **2011**, *59*, 1458–1466.